POTENTIAL VORTICITY PERSPECTIVE OF MODEL VALIDATION

T.Davies
Meteorological Office
Bracknell, U.K.

1. INTRODUCTION

Of the many different ways of validating atmospheric models described during these seminars, none are used in isolation. Most are complementary and each address either one or a range of different aspects. The aim is not just to score the performance of a particular model but also to identify and explain deficiencies in the simulations so that these may be rectified. Those involved in the development of numerical weather prediction models employ an armoury of diagnostic methods in trying to validate their models. This paper describes how potential vorticity maps can give insight into the behaviour and problems of atmospheric models.

In 1985, Hoskins, McIntyre and Robertson (HMR) published a timely and exhaustive review on the use and significance of isentropic potential vorticity maps. McIntyre presented aspects related to cyclogenesis to the ECMWF seminars held in 1987. It appeared to some of us at least that we might be on the threshold of some exciting theoretical developments in the way we view and understand the atmosphere in an operational forecast environment. The reality appears rather more like the collapse of Communism; initial euphoria replaced by chaos and inertia.

It is true that potential vorticity (PV) appears more often in research papers and case studies than before even though the earliest studies date back to the 1940's. However, as far as I am aware, there is no routine operational use of PV and little use in model development. This paper discusses briefly the use of PV in understanding atmospheric flow and development and in particular its use in the validation of model simulations.

2. USE OF POTENTIAL VORTICITY MAPS

The usual definition of PV in isentropic coordinates is given by

$$P = -g (f + \zeta_\theta) \partial\theta/\partial p$$

where f is the coriolis parameter and ζ_θ is the relative vorticity on the isentropic surface θ. $\partial\theta/\partial p$ is a measure of the static stability. The above expression includes only the vertical component of vorticity and the hydrostatic assumption. Ertel's theorem for adiabatic, frictionless motion states that P is conserved following an air parcel. Together with the conservation of potential temperature θ, this provides a means of following air parcels. Moreover, from the distribution of P it is possible to derive other dynamical fields such as winds and temperatures; the invertibility principle. Further details on the derivation of PV and the invertibility principle may be found in HMR.

To use IPV maps, the user needs to recognize that PV (and potential temperature) controls the dynamical evolution of the atmosphere and the theory shows how the distribution and movement of PV controls through

(mutual) adjustment the evolution. To utilise effectively PV maps on isentropic surfaces, two sets of basic concepts are required to establish a framework.

Firstly, some idea of the general vertical structure of the atmosphere in terms of potential temperature is necessary. Figure 1 shows a north-south cross-section from an ECMWF model analysis for 00UTC 13/1/89. The thin full lines are the isentropes (lines of constant potential temperature θ). Average potential temperature cross-sections for January and July which give essentially the same picture may be found in Dutton (1986, pages 92 and 93). The isentropes generally are nearly horizontal (much of the atmosphere is barotropic) except in a region such as the polar front where they slope. The lower stratosphere is evident due to the packing of the isentropes (high stability). Viewing the atmosphere on a particular isentrope may involve changes in altitude. For example, isentropes in the region of 300K to 320K may be found in the lower to mid-troposphere in the sub-tropics but in the lower-stratosphere or upper-troposphere in polar regions. There are three good reasons for using potential temperature in this way. The first is because of the simple definition of PV in isentropic coordinates which essentially reduces to a product of the absolute vorticity and static stability. The second reason is because of the conservation properties of both PV and θ for adiabatic motion which enables us to follow particular structures in PV over a series of charts. The third is that in adiabatic motion, air parcels just follow the isentropes.

Using the above formula for PV we can obtain an idea of typical values in different regions. We note that the PV depends on the static stability $\partial\theta/\partial p$ and the absolute vorticity $f+\zeta_\theta$. Taking a lapse rate of around 10K per 100hPa and absolute vorticity of $10^{-4}s^{-1}$ gives a value of PV around $10^{-6}m^2s^{-1}Kkg^{-1}$ which following HMR is our unit for PV or pvu. In the troposphere the static stability is low and therefore PV is often less than 1 unit there. In the stratosphere the static stability generally increases with height and around the tropopause values of PV of between 1 and 4 units are typical. Areas of large relative vorticity will also show as areas of higher PV but in the troposphere such regions tend to have low stability so that PV in the troposphere will often be lower than 1 unit. Note that in the southern hemisphere PV values are usually negative since the absolute vorticity is usually negative.

A useful concept (attributed to Kleinschmidt) for thinking in terms of PV is of a reservoir of stratospheric high-PV polar air. There is a similarity with the concept of the polar vortex in the stratosphere, itself a region of relatively high PV. Imagine the tropopause as an almost flat-bottomed, bowl-shaped structure centred over the pole. Inside this bowl is our reservoir of high-PV air. If we cut a horizontal section near the base of the bowl the boundary would describe a circle on a polar, stereographic projection. This circle would cover a larger area the further up the bowl we cut our section. In the real atmosphere the bowl is highly distorted, particularly in the northern hemisphere because of undulating Rossby waves and other disturbances. Moreover, the surface of the bowl is not smooth but has protrusions and indentations . Blobs are also present both inside and outside the bowl. This bowl also changes altitude with the seasons; the tropopause rises in the summer hemisphere and descends in the winter. For example, on the 315K surface our PV reservoir (PV>1pvu) occupies around 35% of the northern hemispheric area in the winter and around 10% in the late summer. In the southern hemisphere, the reservoir area in winter is also around 35% but in summer it reduces typically to around 15% of the hemisphere. On the 330K surface the comparable areas are just around 50% in winter for both hemispheres and in summer around 25% for the northern hemisphere and 35% for the southern hemisphere.

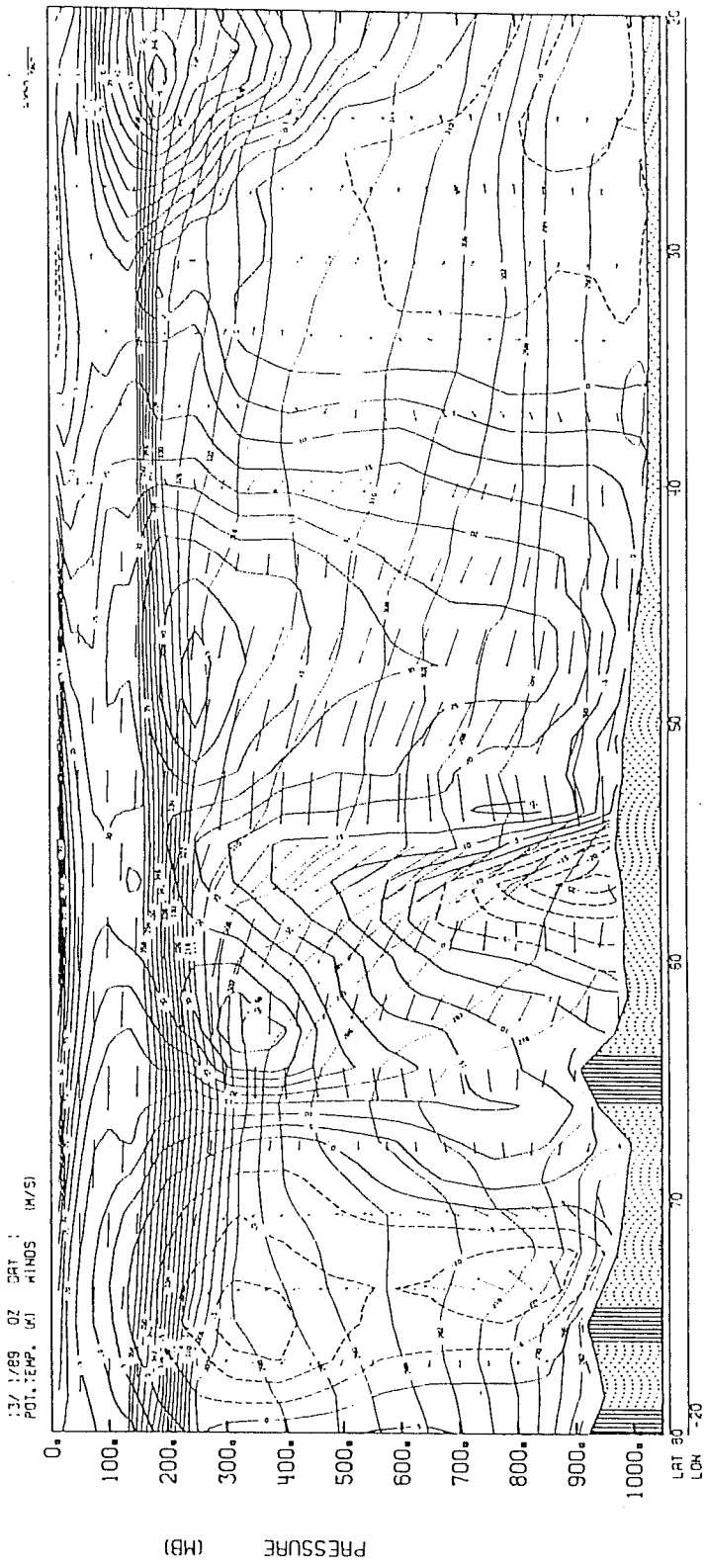

Fig. 1. Cross-section from 80°N to 20°N at 20°W from ECMWF analysis valid 12UTC 13/1/89. Isentropes and westerly wind component, full lines, easterly wind component, dashed line, and North-South-vertical wind component, arrows. The isentropes are only plotted up to 350K. Note that isentropes tend to be horizontal in most regions and are close together in lower the stratosphere indicating high stability. The isentropes slope markedly in the polar frontal zone around 55-60°N.

A PV anomaly is an area of PV which is different from its surrounding values. This may be an area of high PV in a region of relatively low PV or vice versa - the protrusions, indentations and blobs. A large, PV anomaly (positive in the northern hemisphere, negative in the southern hemisphere) induces a cyclonic circulation and causes the isentropes to be raised upwards towards the centre of the anomaly. (See figure 15a in HMR for a picture of an idealised, circularly, symmetric high-PV anomaly originally computed by Thorpe (1985). See also figures 5 to 7 in this paper which describe a close approximation to the idealised solution. The balanced structure also has low surface pressure at the centre.

A low-PV anomaly induces an anticyclonic circulation and causes the isentropes to be pushed downwards away from the centre of the anomaly. (Figure 15b in HMR shows an idealised, circularly, symmetric, low-PV anomaly; also from Thorpe, 1985.) The balanced structure has high surface pressure at the centre.

Equivalent structures exist for low-level potential temperature anomalies. Figure 16a in HMR shows a circularly, symmetric, warm, boundary-layer anomaly inducing a cyclonic circulation and low surface pressure (also from Thorpe 1985). Figure 16b in HMR shows the corresponding cold anomaly inducing an anticyclonic circulation and high surface pressure.

In the real atmosphere, anomalies are not usually circular or symmetric. An equatorward (poleward) extension of high (low) PV would constitute an anomaly as would a blob of (usually high) PV in an otherwise uniform environment. Of particular note are those areas of PV which have the appearance of troughs and ridges (where the terms are used to reflect their counterparts on an upper-air chart) so that a tongue of HIGH PV extending into an area of low PV is termed **trough** whereas LOW PV extending into a high PV area is termed **ridge**. As on height charts, the troughs and ridges sometimes extend and cut-off. As well as the major troughs, ridges, and cut-offs there are other anomalies, particularly of high PV and sometimes almost circular in appearance, which themselves are responsible for development of the flow and in some circumstances may give rise to intensification of pre-existing anomalies as they are advected. PV is also conserved in adiabatic, frictionless motion which means that it is possible to use PV as a tracer of the motion in such cases. In practice, because of friction and other diabatic effects, the conservation is not exact. Nonetheless, quasi-conservation allows features in the PV to be traced forwards or backwards with some degree of success.

In the real atmosphere, the combination of upper (PV) and lower (PT) anomalies can, in some instances, produce dramatic effects; most notably in cyclogenesis events. However, all atmospheric phenomena are controlled in some way by the movement and distribution of these anomalies and synoptic events such as for example, trough disruption, ridge development or blocking, can be observed by looking at a combination of IPV and PT maps although in the latter it is better to include moisture by using θ_e or θ_w instead. Using PV as a tracer in the real atmosphere has its limitations, especially in cases where diabatic effects dominate. Moreover, in most numerical models currently used PV is not one of the variables used. Thus not only does PV have to be diagnosed from other variables but the forward integration of the model does not implicitly maintain the full integrity of the PV due to differencing errors, particularly in the vertical, lack of resolution and dissipation. The diagnosis of PV itself usually involves interpolation and this may also be a source of error. Notwithstanding the above, certain well-defined regions of anomalously high or low values can often be tracked for several days even if the values themselves are changing.

In practice, a suitable isentropic surface for viewing PV is one that intersects the polar-front jet since the anomalies responsible for much of the tropospheric development are more visible there. Such an isentrope will be in the lower troposphere in the sub-tropics and will rise through the polar frontal zone, emerging in the lower stratosphere on the poleward side of the jet (see for example the 310K isentrope in figure 1). There is a slight seasonal variation in the choice of the most appropriate isentrope but usually the 315K surface is adequate for most seasons in the extra-tropics. In the northern hemisphere in summer, 330K is usually more revealing.

Figure 2 shows a stratospheric PV map on the 475K surface, approximately 50hPa from a T+24 ECMWF forecast from 12UTC 19/2/89. At this level the isentropes are almost horizontal. The PV values are contoured every 5pvu with values between 25 and 30pvu shaded. The main stratospheric polar vortex is quite well delineated by the shaded region which is also where the main gradients in PV are. Outside the vortex there are some blobs of higher PV which may have detached from the vortex at some time. At the corners of figure 2 values of PV approach zero near the equator and indeed go negative in the southern hemisphere. This particular case shows the onset of a sudden warming where the vortex is splitting in two and low-PV air is moving towards the pole.

Figure 3 shows the PV map on the 315K surface from the initialized ECMWF analysis valid at 12UTC 1/12/89. PV is contoured every 1pvu with shading between 1 and 2pvu. Also plotted are the winds on the 315K surface and the dashed lines shows the pressure level of the surface at intervals of 50hPa. Generally, the shaded zone follows quite well the meandering jet-stream although unlike a jet-stream analysis which tends to appear discontinuous, the shaded zone is a continuous feature. However, regions of higher PV (cut-offs) are sometimes separated away from the main PV reservoir as is evident for example over the UK. Conversely, regions of low PV can become cut-off from the main source region equatorwards of the jet-stream. The plotted winds serve to give an idea of the instantaneous advection of PV. It must be remembered that the distribution of PV determines the wind (and temperature) so that as PV moves the wind field alters. (However, these changes are not usually drastic enough on the time-scale of interest to obscure the picture of advection.) The pressure levels are useful not only in showing the altitude of the anomalies but also to show the motion up and down the isentropes (up-gliding and down-gliding). From a synoptic point of view these motions may account for the largest contribution to the adiabatic, vertical motion in places. Compared with the previous figure showing the stratospheric vortex, figure 3 appears to have much more structure and complexity. However, this does not preclude us from making use of the PV maps at these levels.

Together with a chart of mean sea-level pressure and equivalent potential temperature at 850hPa (or alternatively wet-bulb potential temperature), a PV map as described above enables one to build up as comprehensive a picture of the structure of the extra-tropical atmosphere that is possible with just two charts. With these we can track the different air-masses, identify frontal zones and follow the main features in the upper-air which are responsible for developments both at the surface and of upper-air features themselves.

A few comments concerning conservation of PV. Using Ertel's theorem, we know that a parcel conserves its PV value under adiabatic conditions. Thus, for example, a parcel in say a shaded region in figure 3 will remain in such a region under adiabatic conditions. Different values of PV are not mixed horizontally thereby producing a dilution of the larger values. However, such a region may itself move and distort so it we may

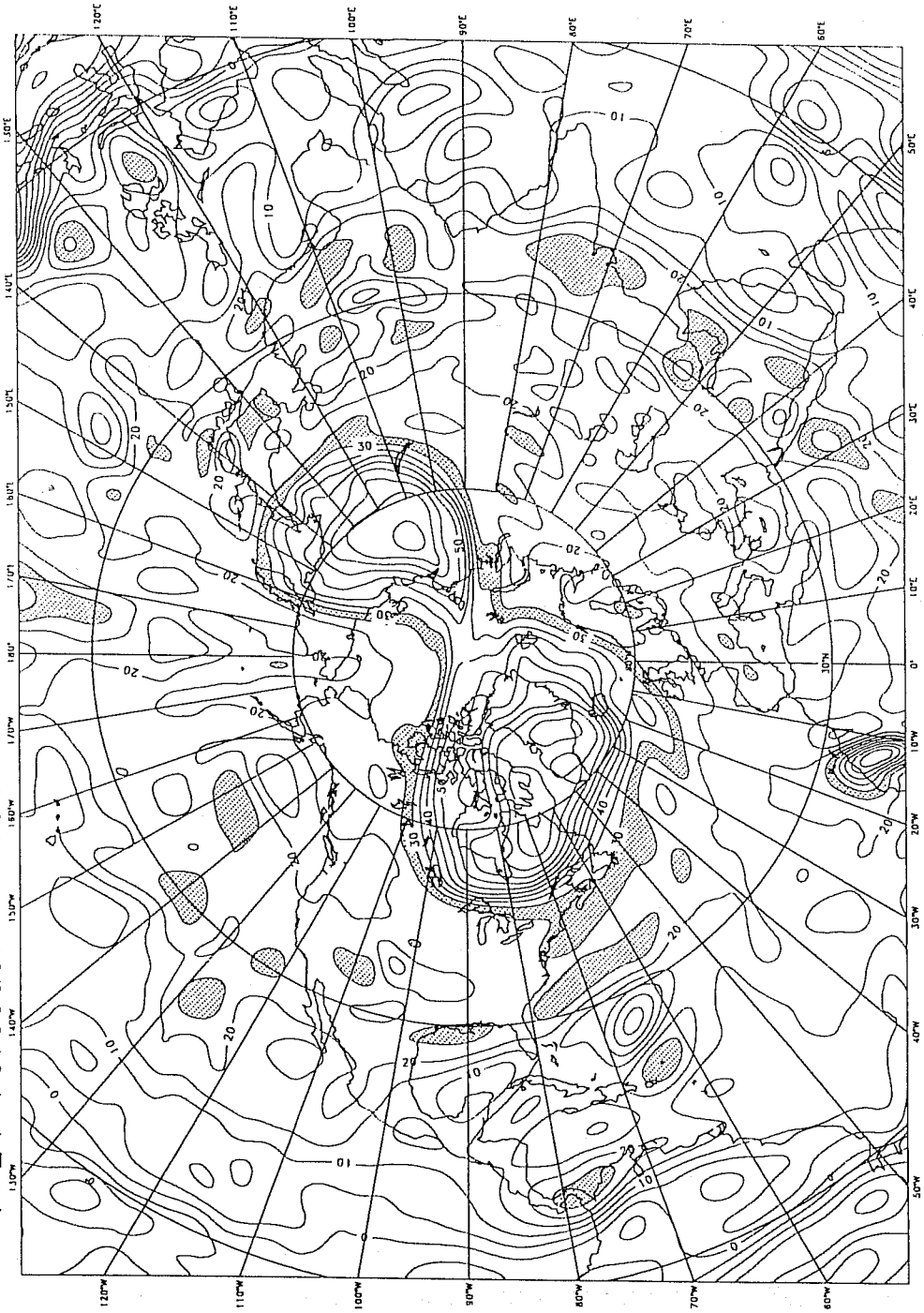

Fig.2. Potential vorticity on the 475K surface (around 50hPa), Northern hemisphere from a T+24 ECMWF forecast from 12UTC 19/2/89 valid 12UTC 20/2/89. PV is plotted every 5 PV units with shading between 25 and 30 units. The stratospheric vortex has a distinct PV signature; well-defined by PV of around 25-30 units. This is the onset of a major warming showing the characteristic splitting of the vortex taking place.

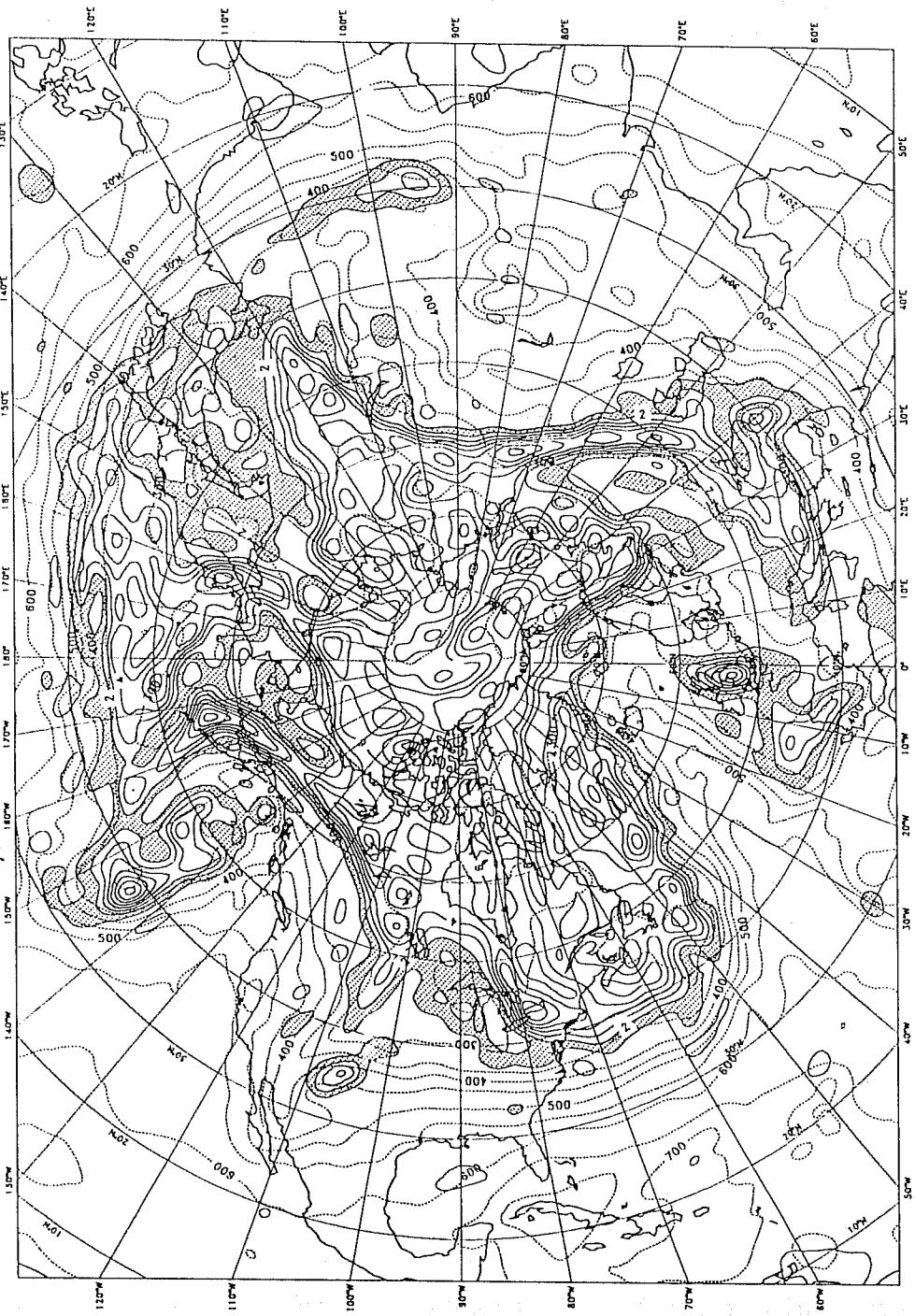

Fig.3. Potential vorticity on the 315K surface of the northern hemisphere from an ECMWF analysis valid 12UTC 1/12/89. PV is plotted every 1 PV unit with shading between 1 and 2 units.

not be able to say exactly where a particular parcel or group of parcels have come from or are moving to. Nonetheless, if there is a significant change in PV at a location, it is often possible to identify from where the parcels responsible for that change came from. Obviously, movement of major troughs and ridges can be followed in this manner as when using height charts. Viewing in terms of PV is particularly useful when troughs (or ridges) amplify as a result of an injection of still higher (or lower) PV. It is also useful when a trough or ridge disrupts or collapses when careful examination of PV maps often reveal the squeezing out or sometimes the isolation of the relevant PV signature by a larger scale movement of PV anomalies.

In a sequence of maps, values of PV associated with a particular feature often appear to be far from conserved. Diabatic processes result in a redistribution of PV such that at a level where there is heating (cooling), PV will decrease (increase) just above and increase (decrease) just below the heating level (see HMR and Hoskins 1990). Furthermore, significant heating or cooling results in a change in potential temperature so a sequence of maps on a particular isentrope might not necessarily follow the same parcels. In a region where there is cooling (heating) the isentropes move upwards (downwards) and will normally sample parcels with larger (smaller) PV. Typically, the most significant diabatic processes are condensational heating from both large-scale and convective precipitation and cooling by radiation, especially from cloud tops.

In a sequence of analyses, apparent non-conservation may be due to inadequacies within analyses where particular features may be missed or wrongly analysed due to missing or incorrect data. In output from numerical models, apparent non-conservation may reveal deficiencies in the modelling process due to errors in particular schemes or excessive diffusion and dissipation. Since most operational NWP do not use PV as a variable, PV maps have to be produced by processing other variables and by the use of interpolation. Small errors in this may also result in errors in the PV values.

The following sections contain examples of different situations illustrating the various signatures and behaviour associated with PV anomalies. Each section is designed to give an insight into the particular event in a similar way to that obtained by a study of the standard outputs, such as a sequence of height charts, and not as an investigative case study of the particular situation.

The following sections show the use of PV in different synoptic situations in order to help the reader develop a feel for what to look for. PV signatures for troughs, ridges, cut-off highs and lows and how their movement and interaction elucidate our understanding will also be discussed.

3. ISOLATED CIRCULAR ANOMALIES

Figure 4 shows the 315K PV map from an ECMWF analysis for 12UTC 1/12/89. The contours are every 1 pvu with shading between 1 and 2 units. The dashed lines show the altitude (pressure level) of the 315K surface which is at around 700hPa in the sub-tropics and above 300hPa in the Arctic. Note the gradient in the altitude is almost parallel to the 1-2 unit shaded area which meanders around the hemisphere. This is the polar front jet. Areas of PV have detached from the main reservoir of PV and one such area is over the UK. It is almost circular in appearance with a maximum value in excess of 7pvu. The circulation around the anomaly is cyclonic as may be discerned from the wind arrows.

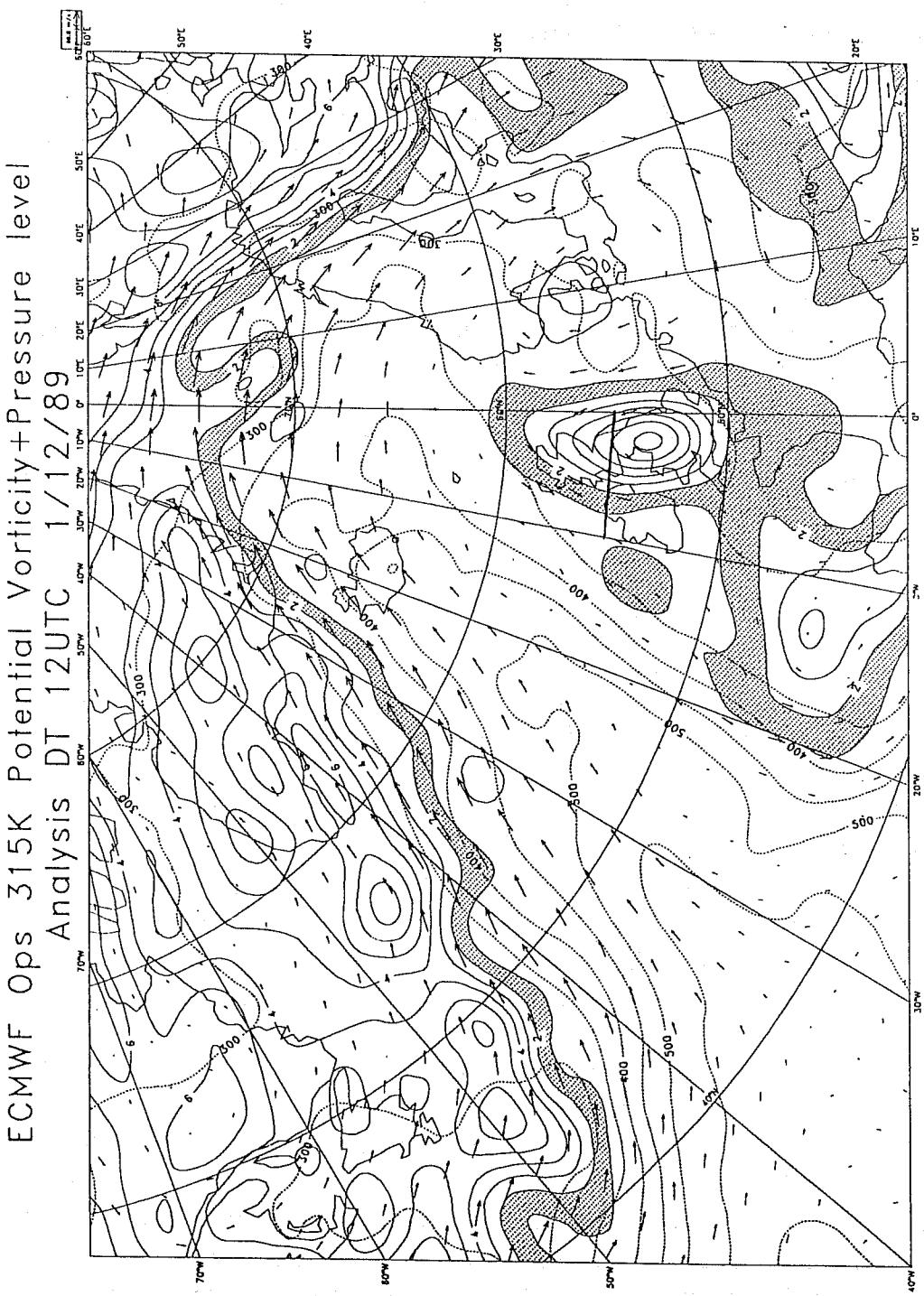

Fig.4. As figure 3 but zoomed-in on Northwest Europe and the Northern Atlantic. Wind arrows on the 315K surface are plotted together with the altitude (pressure level) of the 315K surface (dotted line).

Figures 5 and 6 are cross-sections along 55° north between 10° west and the Greenwich meridian as indicated by the dark line on figure 4. Figure 5 shows PV in units of 0.2pvu up to 5pvu with 1, 2 and 5pvu highlighted. If we consider the 300hPa level, then the PV is about 1.5pvu on the left, increases above 5pvu in the centre and decreases to below 1pvu on the right. Figure 6 shows the corresponding isentropic and wind structures associated with this anomaly. The isentropes are the thin lines across the picture which appear to be bowing upwards in the middle. The southerly wind component (into the paper) is shown by the full lines with the maximum of $35ms^{-1}$ highlighted. The northerly wind component (out of the paper) is shown by the dashed lines with the maximum of $25ms^{-1}$ highlighted. The wind arrows show the east-west and vertical components. The cross-sections bear a strong resemblance to the "idealised" solutions obtained by Thorpe (1985) and reproduced in HMR. The asymmetry in the wind is due to the departure from circular symmetry of this real PV anomaly.

Figure 7 shows figures 5 and 6 superimposed to reveal the relationship between the wind maxima and the "tropopause" defined as 1-2 pvu. The characteristic sucking upwards of the isentropes results in a reduction in static stability below the anomaly. Furthermore, as adiabatic flow is along the isentropes, any component of the wind towards (away from) the centre of the anomaly will take air parcels upwards (downwards) along the isentropes relative to the movement of the anomaly, which in this case is small. In a reference frame moving with the (non-developing) anomaly, the isentropic up(down)-gliding gives the adiabatic part of the vertical motion.

4. ANTICYCLONES AND CUT-OFF LOWS

A strong, poleward jet has long been recognised as one of the conditions leading to the formation of a blocking anticyclone. Such developments have a distinct PV signature. Crum and Stevens (1988) published a case study of atmospheric blocking in terms of PV. An alternative example is produced here.

Figure 8 shows a sequence of ECMWF analyses of PV and winds on the 310K surface for 12UTC on 16, 17, 18 and 20th January 1988. PV is contoured every 1pvu starting at 1pvu with 1-2pvu shaded. South of Iceland on 16/1/88 there is a strong southerly jet transporting low-PV (<1pvu) air polewards ahead of a trough of high-PV air. There is an area of low-PV air over the Icelandic region which is developing an anticyclonic circulation. The northerly winds on the eastern side of the ridge are weaker than those of the southerly flow to the west suggesting that there is an accumulation of low-PV air in the anomaly or ridge.

In this case the trough to the west is moving eastwards and by 12UTC 17/1/88 the high-PV air has isolated the low-PV air from its source region. By this stage the low-PV anomaly is circular and it has a well-developed anticyclonic circulation. The low-PV air cannot mix horizontally with the surrounding high-PV values. Instead it will keep its identity unless either the PV increases through (vertical) diabatic effects, such as radiational cooling, which in this type of situation are slow and result in increases of about 1pvu in 5 days (see HMR, section 7), or if it joins to another region of low-PV. Typically this can occur if there is another ridge building upstream which then amalgamates with a pre-existing anomaly giving the appearance of retrogression of a blocking high or, as in this case, the anomaly drifts slowly back towards its sub-tropical source region which can be seen in the frame for 12UTC 20/1/88 where the anomaly has almost joined back to the low-PV air near 40°N 80°E.

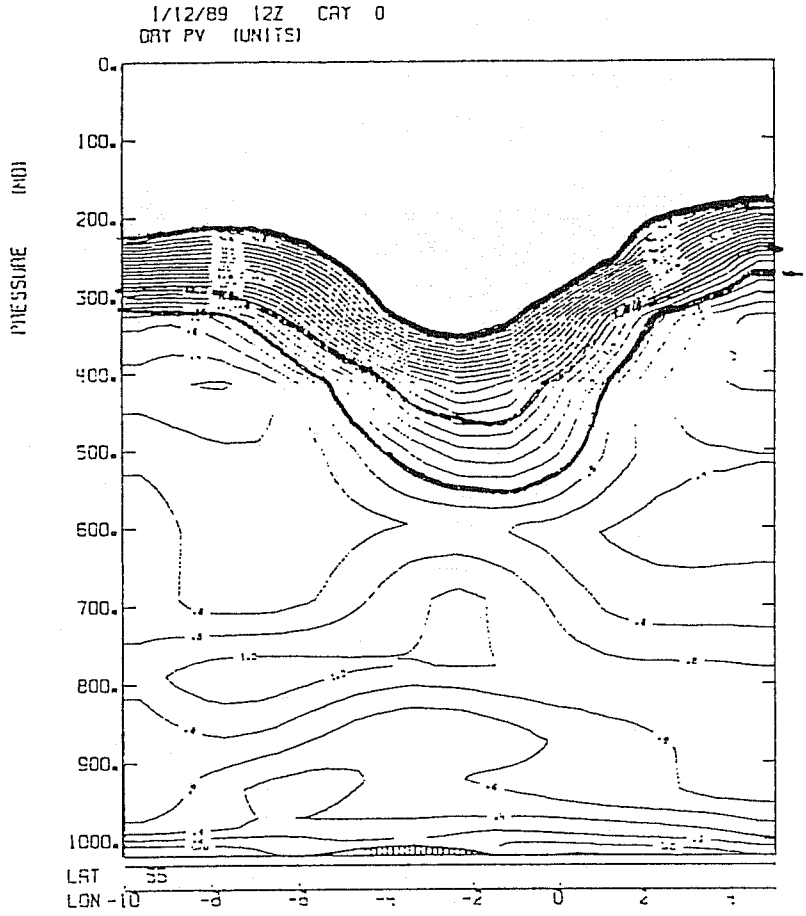

Fig.5. Cross-section through isolated PV anomaly shown over the UK in figure 4. Section is at 55°N from 0-10°W. PV every 0.2 units up to 5 units with 1, 2 and 5 units highlighted in the lower stratosphere.

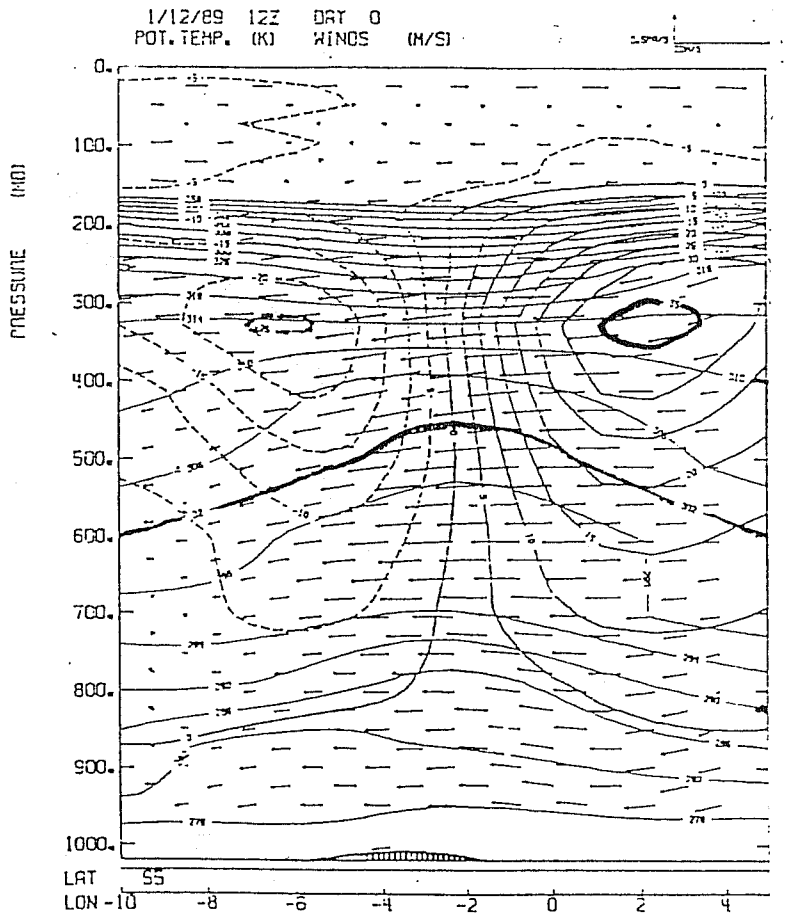

Fig.6. As figure 5 but showing isentropes every 4K (solid line, 302K highlighted), southerly winds every 5m/s (solid line, 35m/s highlighted), northerly winds every 5m/s (dashed line, 25m/s highlighted) and East-west-vertical wind components (arrows). See text for explanation.

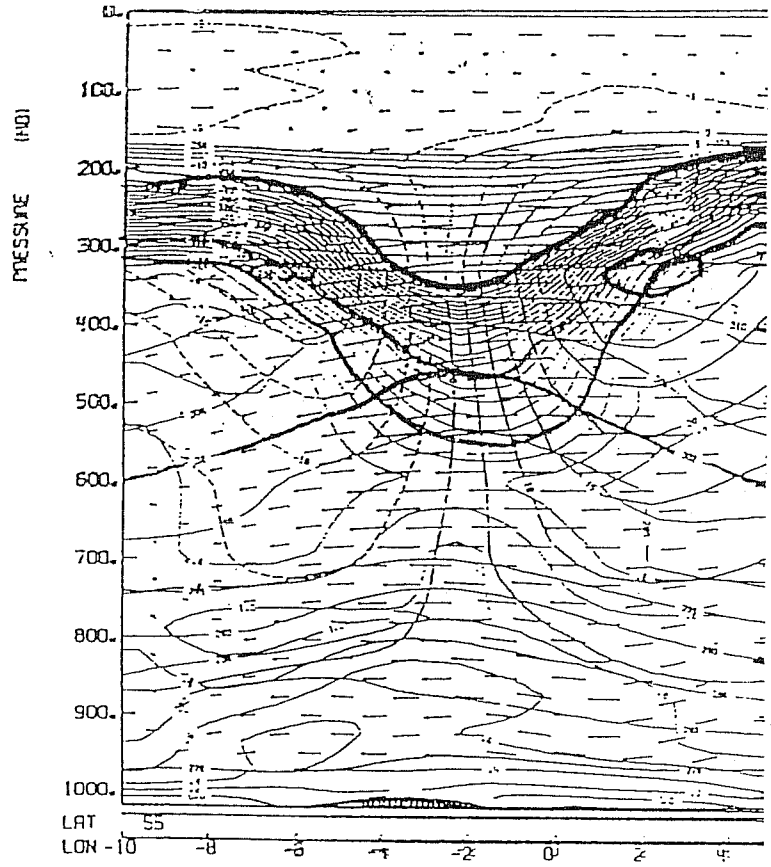

Fig.7. Combination of figures 5 and 6 showing the relationship between the PV, isentropes and winds.

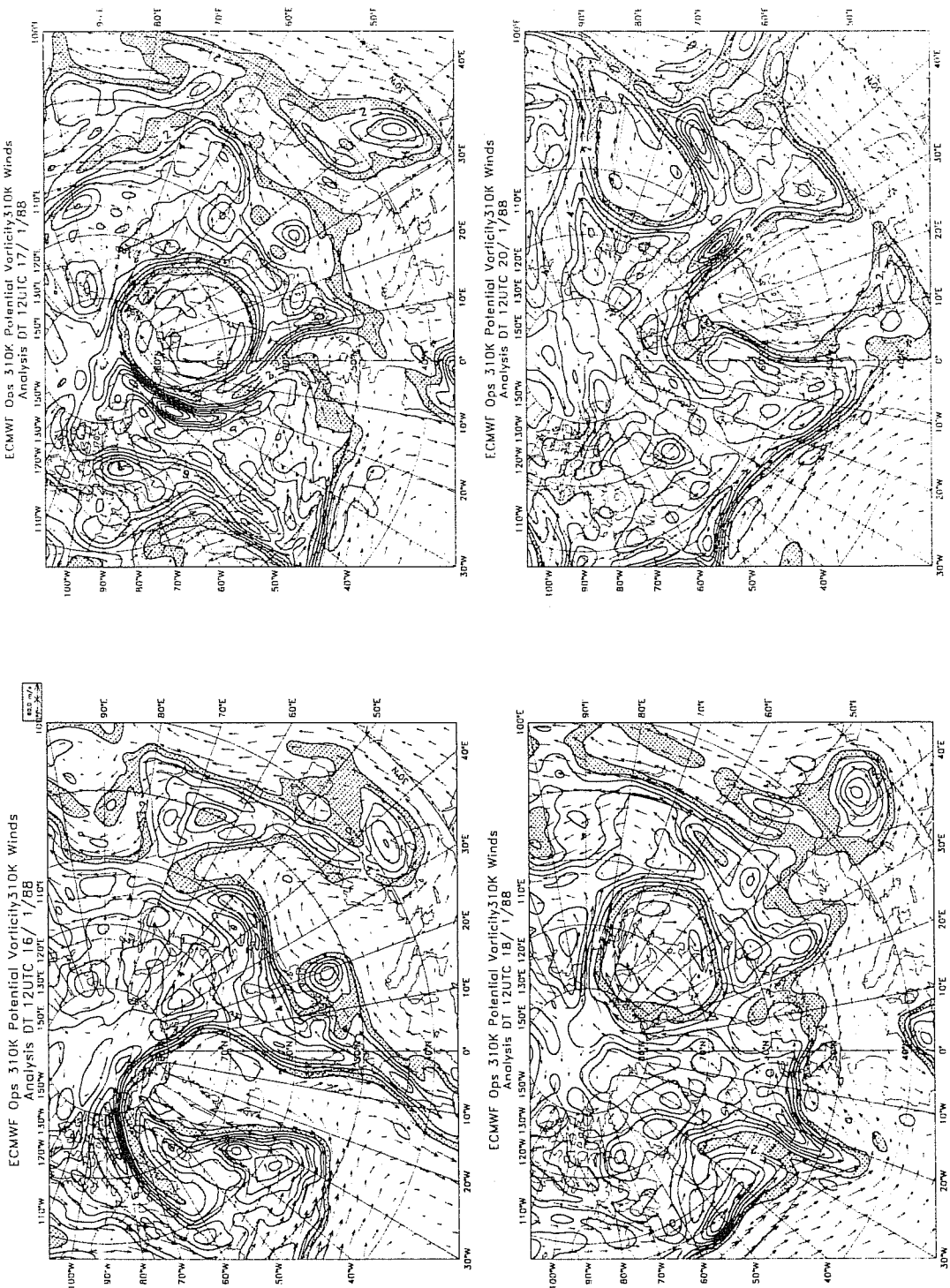

Fig.8. Sequence of 310K PV and winds from ECMWF analyses valid at 12UTC on 16, 17, 18 and 20 January 1988. See text for details.

Trough extension and retrogression (Miles, 1959) may also be viewed in terms of low-PV anticyclonic development. In the top-left frame in figure 8 for 12UTC 16/1/88, the flow on the eastern edge of the building anticyclone or anomaly is southwards in both the low-PV air and in the adjacent high-PV air. Thus high-PV air is transported equatorwards around the ridge, maintaining or reinforcing the downstream trough. Depending on how well developed the anticyclonic circulation is, the transport of high-PV air may also have a westward component resulting in retrogression of the downstream trough.

Cut-off lows are produce when high-PV air is transported equatorwards and becomes detached from the reservoir. Two examples can be seen in figure 8. At 12UTC 16/1/88, two regions of high-PV air have been advected across Iberia and Asia Minor. In both cases, the links to the reservoir are becoming narrow because of the various anomaly-induced circulations and by 12UTC 17/1/88 the anomaly over Southern Iberia is detached, and the eastern cut-off has a weak link east of the Caspian Sea. These cut-off lows or anomalies have similar structure to that of the isolated anomaly discussed earlier. Diabatic processes, in particular warming due to convection can modify (warm out) the anomaly on a shorter time-scale than does radiational cooling on a low-PV anomaly. Depletion rates of 1 or 2 units a day are typical (see HMR, section 7) so that a cut-off low of say 7pvu initially may persist for a few days or up to about a week depending on the intensity of convection. In the cut-off process just described, the low-PV air plays an essential rôle, as its arrival produces the familiar ridge or anticyclone associated with the so-called anticyclonic disruption of the trough.

This particular case illustrates two of the contrasting types of anticyclonic development. The first is the poleward transport of low-PV ahead of a trough and its subsequent isolation as the trough moves eastward. The second is the elongation of high PV equatorwards followed by a break in the link with the high-PV reservoir and the replacement in the region of the link of high-PV by low-PV air.

5. VORTEX INTERACTION

In fluid mechanics, the way vortices interact is known to depend on their size, their separation and the regime. In the real atmosphere, vortex interaction is often observed but it is rarely used as a means of describing a synoptic situation.

Figure 9 shows a series of analyses from 12UTC 17/11/91 to 19/11/91 showing two distinct PV anomalies interacting. On the 17/11/91 (top left) there is a PV anomaly to the west of Ireland associated with a frontal system indicated by dashed lines showing 850hPa θ_e. 12 hours later the anomaly is centred over North Wales with another distinct anomaly north of Scotland. The two anomalies are separated by a region of PV<1pvu. The latter anomaly was south east of Iceland at 12UTC 17/11/91. A further 12 hours later, at 12UTC 18/11/91 the first anomaly is over the North Sea and the second anomaly is moving towards Northern Ireland. The anomalies are now separated by PV<4pvu but their centres are still discrete. After another 12 hours, the first anomaly is over Southern Scandinavia whilst the second is over the Southern Britain.

The same sequence is shown in terms of 500hPa charts in figure 10. Notice how much less significant the first anomaly appears over Southern Britain at 00UTC 18/11/91 (top right) and subsequently as the second anomaly begins to dominate the picture. In terms of height and the thermal field (not shown) it is difficult to envisage what the adiabatic forcing of the vertical motion would be. Obviously, a vorticity chart would

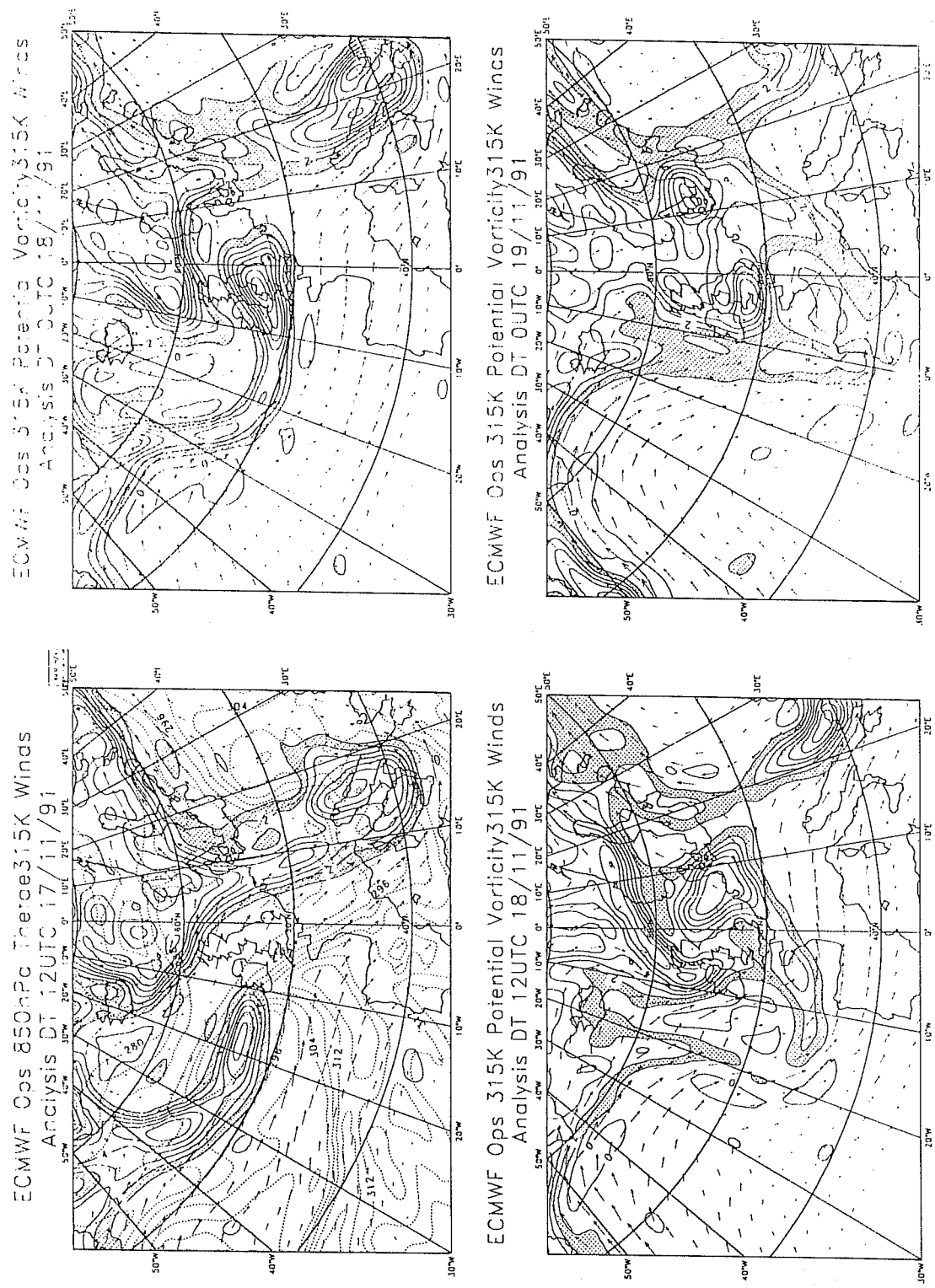

Fig.9. Sequence of 315K PV and winds from ECMWF analyses valid at 12UTC on 17/11/91, 00 UTC and 12UTC 18/11/91, 00UTC 19/11/91. First frame also includes 850hPa θ_e. See text for details.

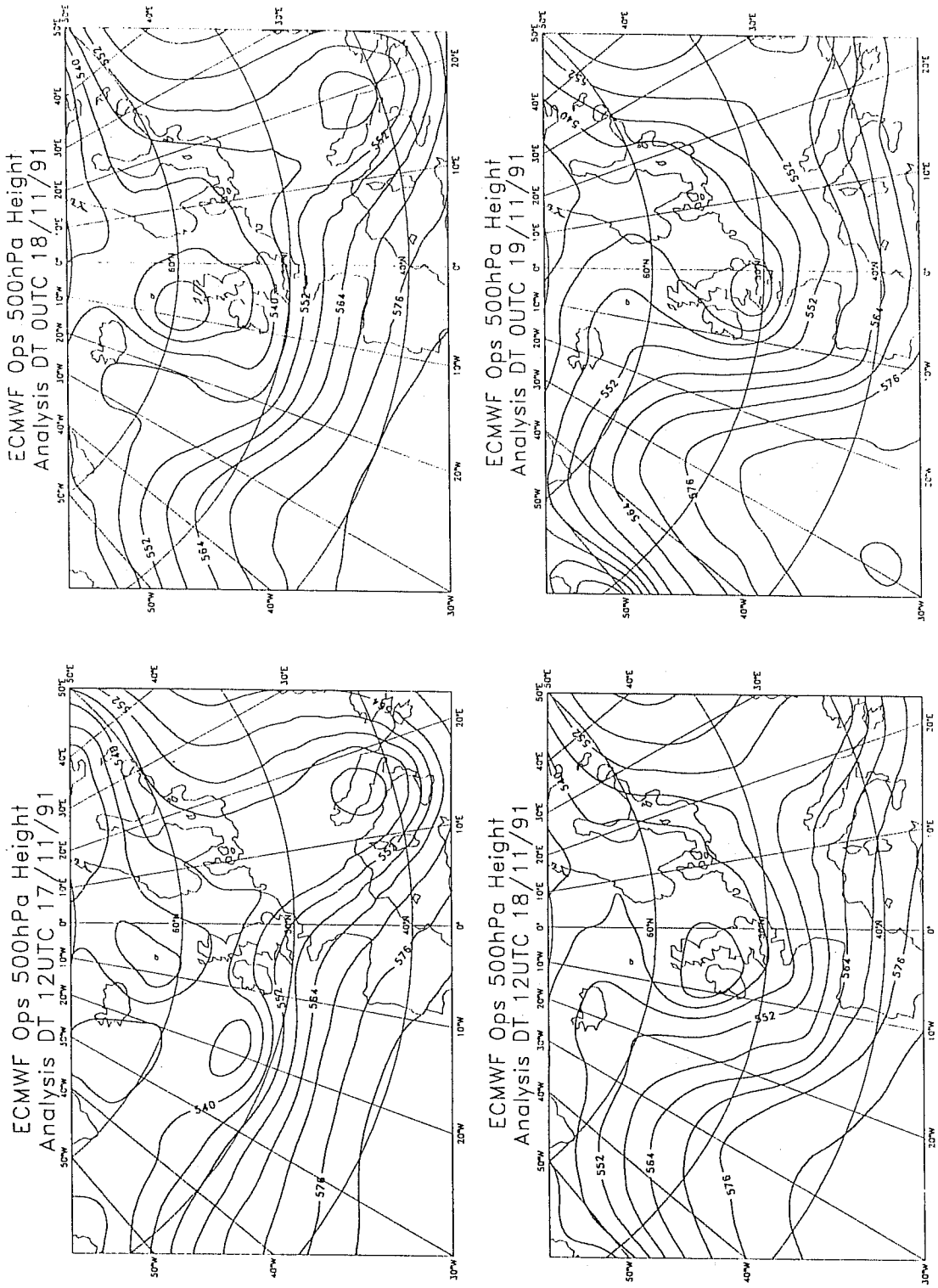

Fig.10. As figure 9 but 500hPa heights.

show the vorticity advection contribution similar to that shown by the PV. However, from the PV picture we are also able to envisage the isentropes and together with the low-level flow (not shown) it is possible to build up an approximate picture of the ω field at say 850hPa.

6. RAPID CYCLOGENESIS

Hoskins et al (1985) produced a schematic picture of cyclogenesis (their figure 21) which describes the arrival of an upper PV anomaly over a low-level, frontal zone. The cyclonic circulation induced by the upper anomaly leads to a warm anomaly near the surface slightly ahead of the upper anomaly. The warm anomaly induces its own cyclonic circulation which may lead to a reinforcing of the upper anomaly.

A high PV anomaly implies a cyclonic circulation and this circulation extends below the anomaly as in figure 6 and in figure 15(a) in HMR. The lower level cyclonic circulation advects warm air towards cold air just ahead of the upper anomaly and in this manner produces a warm boundary layer anomaly (a "bump" of warm air into the cold air). The low-level, warm anomaly itself generates a cyclonic circulation (see figure 16(a) in HMR) and this circulation extends upwards. The induced upper circulation, being just ahead of the upper anomaly tends to advect low-PV air towards high-PV air ahead of the original upper anomaly and advects high-PV air towards low-PV air in the region of the anomaly. This process effectively augments the upper anomaly and slows down its progression. Development may be further enhanced by the advection of yet more high-PV from the reservoir into the anomaly; part of this process involves the jet-streak or vorticity maximum recognised by synopticians.

The above does appear to be a realistic description of the onset of cyclogenesis in the real atmosphere. In some circumstances cyclogenesis can be initiated by low-level anomalies (minor waves on pre-existing frontal zones). Any perturbation in the low-level wind field that produces a warm anomaly will then lead to a cyclonic circulation as described above. However, unless the anomaly can be sustained by a continuing supply of warm air, diabatic processes will rapidly reduce the anomaly; more rapidly than they reduce an isolated, upper anomaly. It may be possible that if the anomaly lies near the edge of the PV vortex then the induced circulation could draw high-PV air aloft towards the development thereby leading to reinforcement in a similar way to the scenario described above. Cyclogenesis is initiated more often by upper PV anomalies rather than low-level, warm anomalies primarily because advection is greater at higher levels; the upper anomalies move about more and are more likely to meet a low-level frontal zone. Moreover, the quicker the movement of the anomalies, the stronger the development which also accounts for the tendency of major cyclogenesis to occur in winter when jet speeds are greater.

Although the above gives a reasonable explanation of cyclogenesis, it is difficult to quantify the deepening of a cyclone by just considering the upper and lower anomalies. The degree of development is influenced by the size (strength) of the anomalies, the speed at which they approach or come together and the (moist) static stability of the troposphere. The strength of the upper anomaly and its speed are related to the familiar quasi-geostrophic concept of positive vorticity advection (PVA).

7. HEIGHT DIFFERENCE MAPS AND PV

Member states occasionally bring the Centre's attention to forecasts which have large errors locally. One such example here relates to a forecast which at day 5 is misleading near Italy. Figure 11 shows a 5 day sequence of analyses (left panels) of PV on the 315K surface for the North Atlantic and adjacent areas from 11/10/89 to 15/10/89. These maps are contoured every 2pvu apart from the 1-2pvu range which is shaded. The right-hand panels show the corresponding forecast sequence from 12UTC 10/10/89. At 12UTC 15/10/89 (bottom left) the analysis shows an extended trough from Scandinavia to the Adriatic and a region of high-PV extending from near Newfoundland to the Faroe Islands. The 5 day forecast (bottom right) has a trough near the Greenwich meridian and a major ridge centred at around 20° west. Figure 12 shows the starting analysis PV map for 12UTC 10/10/89 and in investigations into this forecast error, attention was focused on a deep trough over the Great Lakes which was seen to involve large analysis increments. The PV anomaly over the Great Lakes has a value in excess of 6pvu. Notice that this situation is quite complex in terms of PV structures in that there are several anomalies as the hemispheric flow is disturbed.

There are several significant events indicated by the analysis sequence in figure 11. In the region of Iceland, initially low PV air is replaced by high PV air from the north and west by 12UTC 12/10/89 (second panel down on left). At the same time, the anomaly that was over the Great Lakes on 10/10/89 has cut-off near Nova Scotia whilst a further region of high PV is advancing towards the Great Lakes building a ridge ahead (low-PV air is being advected polewards). Compared with the T+48 hour forecast on the right, there are differences in the detail in the high-PV region over the Northern Atlantic, the cut-off anomaly south of Nova Scotia is displaced southwards and weakened (mostly off frame) and the upstream ridge and trough have different detail. These differences in detail grow so that on 13/10/89, as well as the differences north west of the UK, the ridge over the Davis Straits and the trough extending southeastwards across Nova Scotia are quite different in the T+72 hour forecast. The cut-off anomaly has a displacement error of a few degrees but it is weakening in both the analysis and forecast. One day later and the differences are large. In the forecast for 14/10/89 the flow is essentially a deep trough over Newfoundland, an amplifying mid-Atlantic ridge and an extending trough over the UK. In the analysis, high PV air is moving eastwards across the Atlantic isolating the low-PV air to the north. Since there is little building of low-PV air to the west of the UK, the downstream trough does not extend as much as in the forecast and it has moved further east. A building of the ridge does take place during the next 24 hours as the high-PV air extends northeastwards to the north of the UK and the trough extends towards the Adriatic. The low-PV air (anticyclone) over the Davis Strait is completely cut-off. In the T+120 hour forecast the trough-ridge-trough pattern from the previous day has amplified and moved eastwards.

The same sequence of analyses and forecasts for the 500hPa height is shown in figure 13. The evolution of the forecast error can be tracked to some extent by following the error growth as measured by the difference between the forecast and analysis height charts. These appear in figure 14.

The 500hPa difference maps are useful in highlighting the phase and amplitude differences between the analyses and forecasts. The overall size of the differences generally get larger during the forecast as the errors grow and often it is possible to trace backwards the evolution of the error over at least part of its development. However, many errors grow from perturbations which may still be small during the early part of the forecast and which become evident only after a few days.

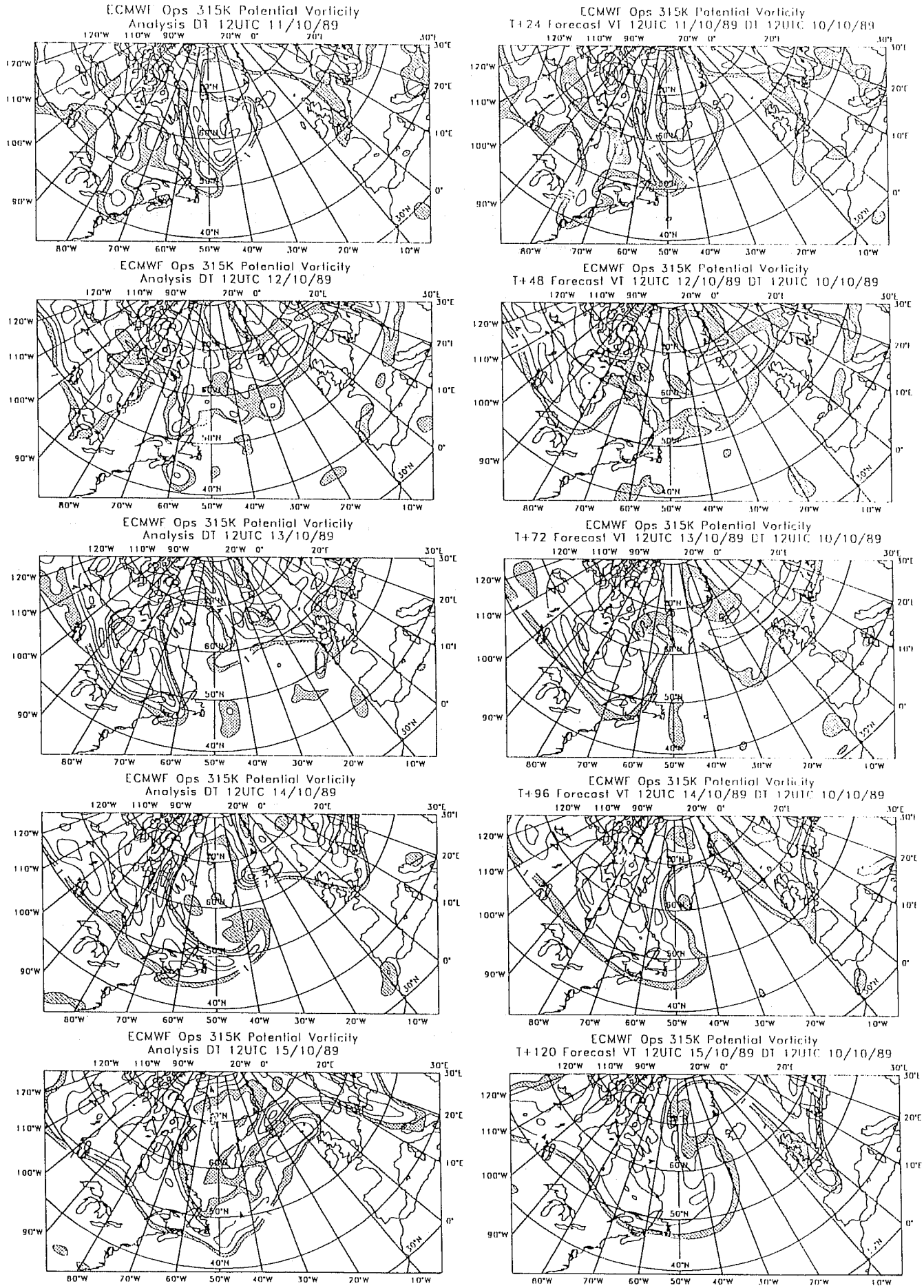

Fig.11. Sequence of PV on 315K surface in region of Northern Atlantic. PV contoured for 1 to 2 units (shaded) and then every 2 units. Left-hand side shows sequence of analyses every 24 hours from 12UTC 11/10/89 to 15/10/89. Right-hand side shows corresponding forecast sequence from 12UTC 10/10/89 valid at the same time as the analyses opposite.

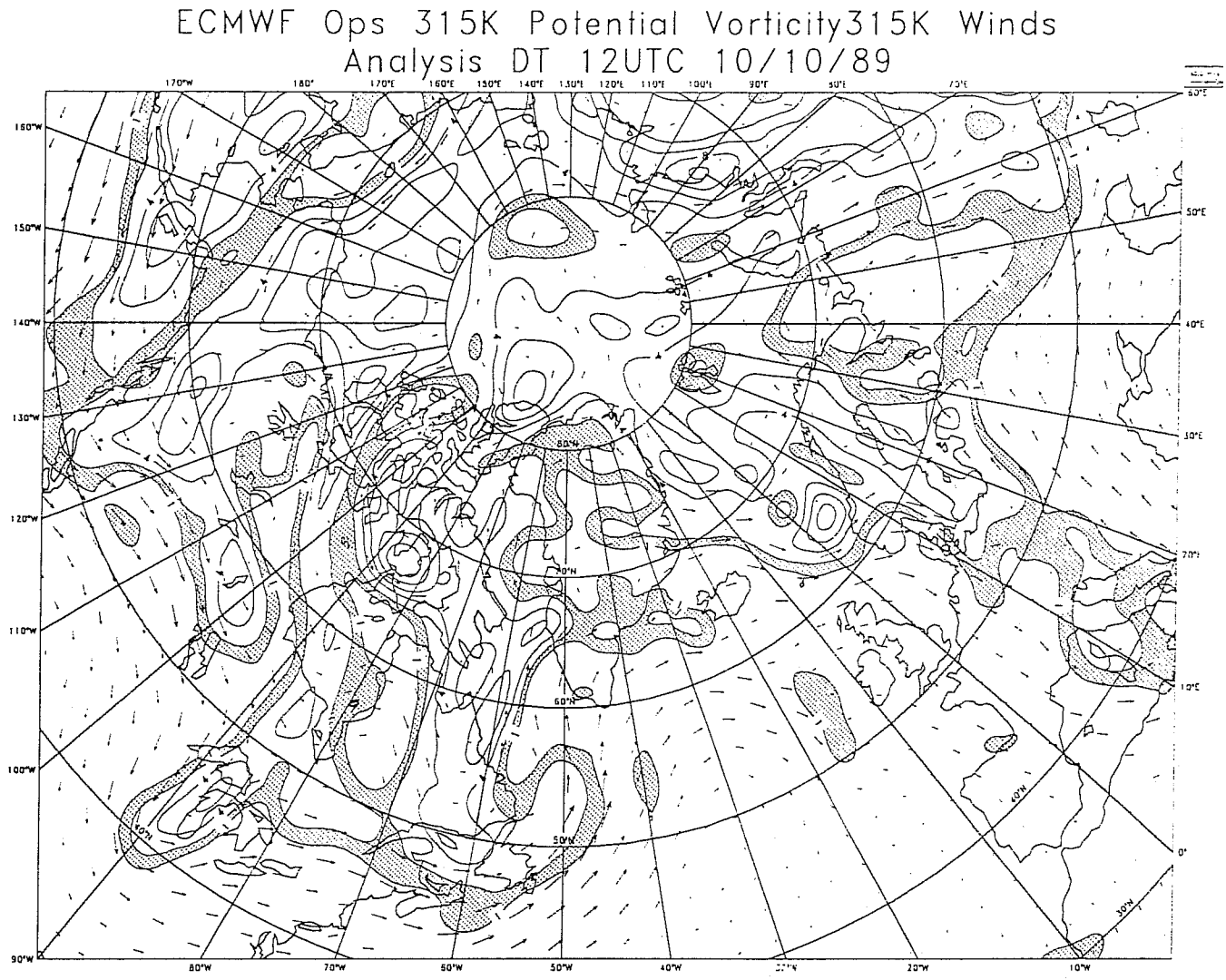

Fig.12. PV and winds on the 315K surface for a similar region as figure 10 showing the initial PV distribution at 12UTC 10/10/89. PV contoured for 1 to 2 units (shaded) and then every 2 units.

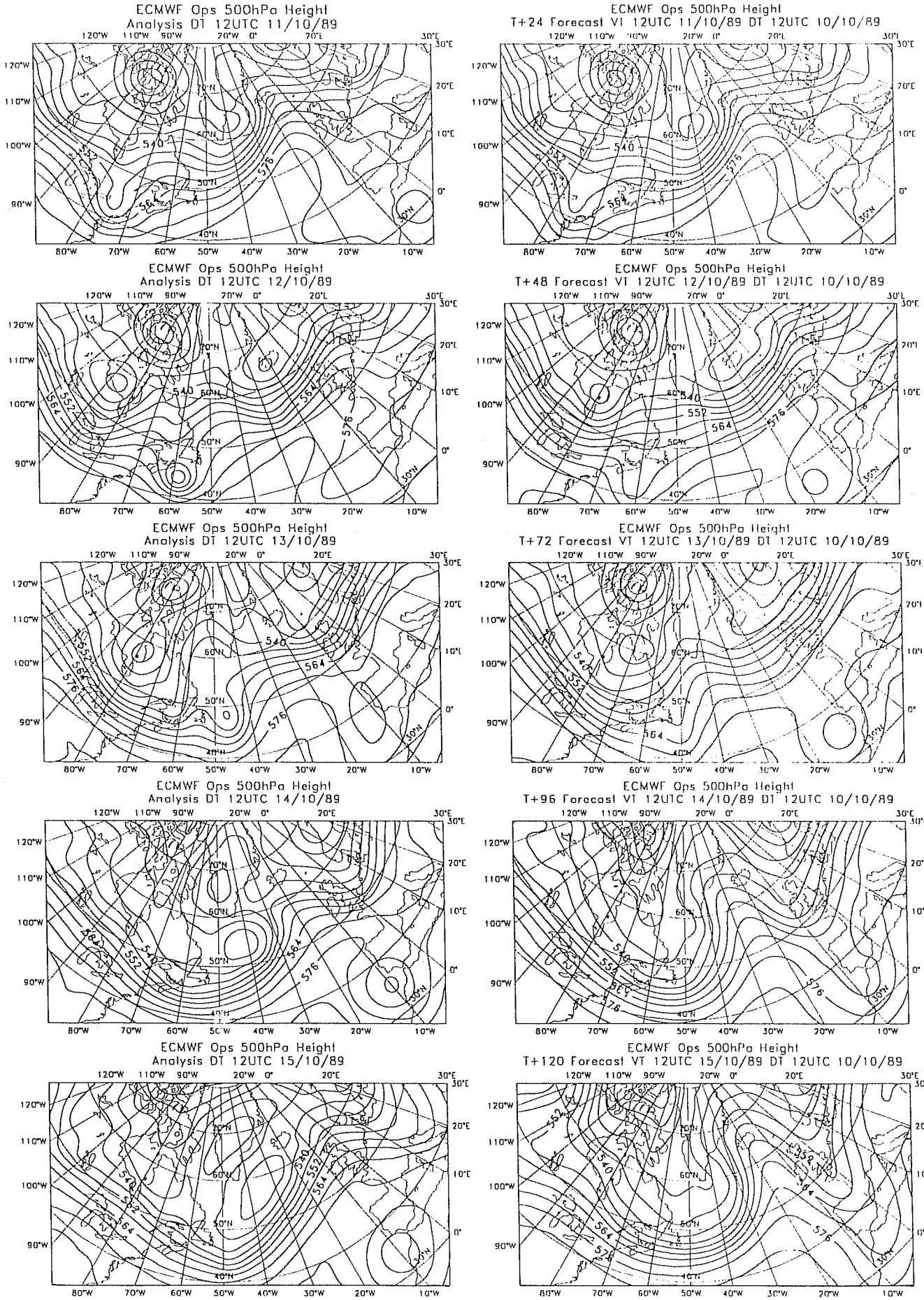

Fig.13. 500hPa height sequence corresponding to figure 11.

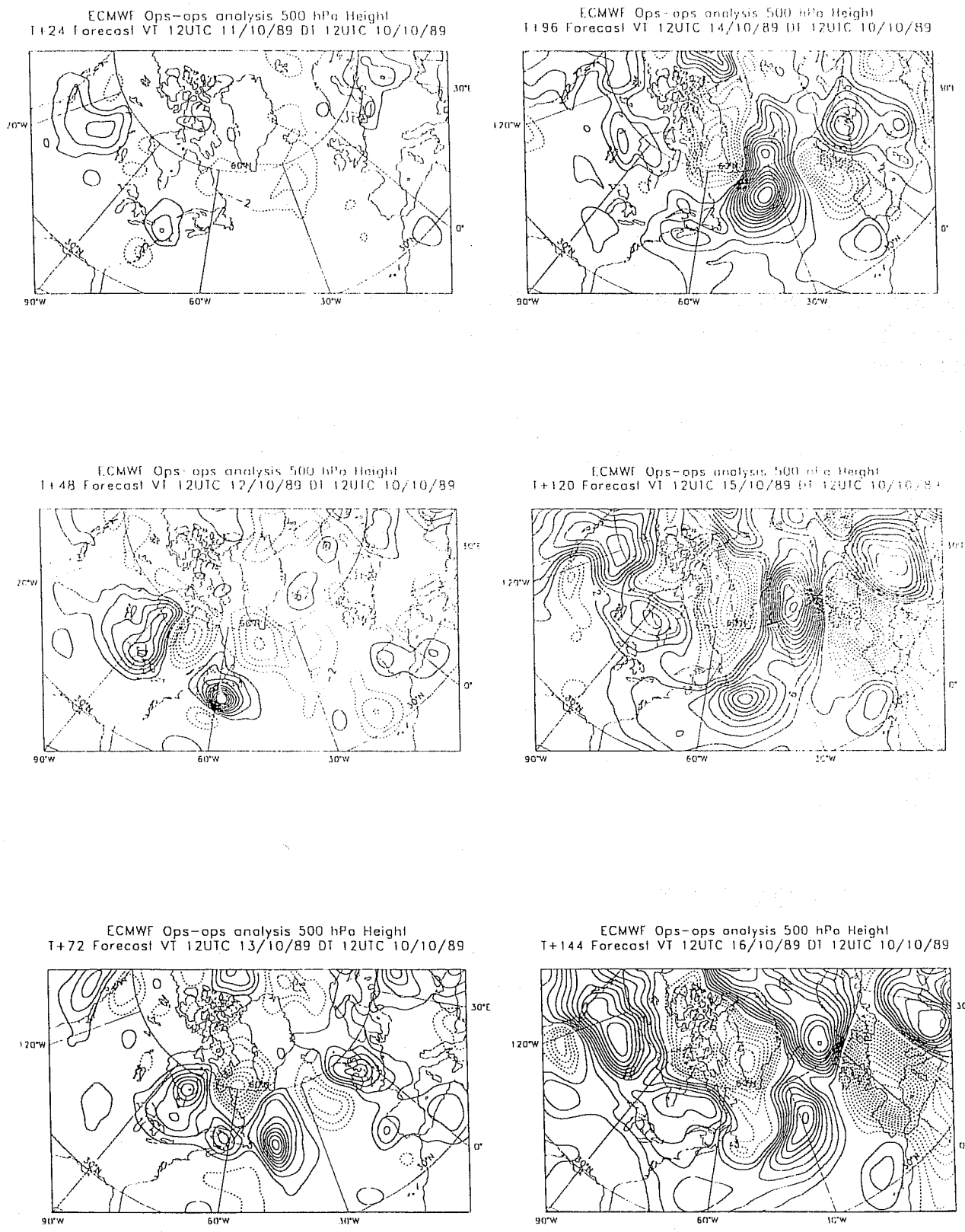

Fig.14. 500hPa error maps (forecast-analysis) for the 6 day forecast from 10/10/89. Contours every 2 Dkm, dashed negative.

In this case, the error associated with the cut-off which started over the Great Lakes can be seen to grow during the first 3 days of the forecast. The errors associated with the mishandling of the upstream and downstream troughs and ridges also grow. By T+96, there is a large error over the mid-Atlantic reflecting errors in the development described above. The height and associated difference maps appear to show that this error evolves from a growth in the error from the previous day. However, it is much clearer when viewing the potential vorticity sequence that it mainly evolves from the apparently smaller error over Nova Scotia at T+72 (12UTC 13/10/89) which is associated with the leading edge of the major anomaly over Eastern Canada. Given the relative magnitude of the cut-off anomaly compared with that of the major anomaly it would seem that the errors in the cut-off play a relatively minor rôle in the failure of this forecast to correctly predict the eastward propagation of the major anomaly and the cutting-off of the low-PV air to the northwest.

As to the error in the forecast of the trough over the Adriatic at 12UTC 15/10/89, the PV evolution in the general vicinity of Iceland between 10/10/89 and 13/10/89 is complex since there is considerable detail in the PV structure and there is probably a certain amount of interaction between the anomalies. However, the original Great Lakes cut-off does not appear to play an important rôle in this either.

This particular example has been used to illustrate how, by considering the PV evolution, a clearer and more direct picture of those features controlling the developments can be made. In this case, a feature which appears to be important when using more traditional diagnostics, is seen to be of less dynamical significance in the PV framework. However, a little care should be exercised in just considering the anomalies alone. The associated wind field may have a significant if subtle affect on the larger scale wind field which advects the anomalies about. In this case the different behaviour of cut-off anomaly between the analyses and forecasts leads to differences in the larger-scale wind field which may have some effect on the movement of the anomalies downstream.

8. MODEL INVESTIGATIONS

Development (hopefully leading to improvements) of numerical models requires assessments of models to be made and comparisons made with other versions and/or models. A major factor in comparisons involves making objective scores of various parameters over different regions, e.g. 500hPa height over the Northern hemisphere, 200hPa winds in the tropics, etc. However cases chosen may not be representative and performance may be better in one region or of one aspect but worse in another. Normally, to get an accurate assessment many cases need to be run and samples need to be from different seasons. Systematic errors are also compared, e.g. the zonal mean temperature error averaged over say the second half of a forecast can show if there are problems or deficiencies in a model. Many other aspects of model validation will be discussed in these seminars. However, even with all these tools, evaluation and interpretation is difficult.

As intimated above, a thorough evaluation involves many runs of a model. Frequently, initial experimentation can be dogged by coding or formulation errors, and these need to be discovered before too much investment is made in testing. Again, the various techniques alluded to above can be employed, but model deficiencies have to be inferred from a relatively small number of cases. Gross errors may be obvious but even quite substantial problems may be difficult to uncover.

PV maps have recently been used as part of ECMWF's model evaluation process and has given useful extra insight into model problems. Figure 15 shows a comparison of 330K PV for the northern hemisphere between analyses and forecasts from the then T106L19 operational model (top panels) and the then experimental T213L31 model (bottom panels). The analyses valid at 12 UTC 21/7/91 are on the left and the 5 day forecasts valid at 12UTC 26/7/91 are on the right. It is clear that T106L19 loses amplitude and that the PV gradients weaken during the forecast. T213L31 also shows a smoothing in the forecasts but the amplitudes and gradients are better maintained. Defining PV>1pvu as the vortex, calculations show that the area of the vortex decreases from 23% of the hemisphere to 20% over the 5 day forecast at T106L19 but increases to 24% at T213L31. We also notice a marked reduction in those areas with PV greater than 3pvu in the 5 day forecast at T106L19. This apparent reduction in PV suggests either a region of (diabatic) warming below 330K (around 300hPa in the vortex) or a region of cooling above. Zonal mean temperature errors, meaned over days 5 to 10 in figure 16 (bottom panel) do indeed show a marked cold bias in the northern hemisphere centred on 200hPa, just above the region of the PV loss. Zonal mean temperature errors at T213L31 (middle panel) show a different error profile with a less intense cold bias spread over a greater thickness. The difference between the T213L31 and T106L19 zonal mean temperature is shown in the top panel of figure 16.

The zonal mean temperature errors just described do not on their own imply that the biases arise from particular processes. Diabatic cooling towards the poles is compensated by adiabatic warming and a stronger diabatic cooling may result in larger adiabatic warming giving a smaller net temperature bias. Figure 17 shows the zonally averaged temperature changes from the diabatic processes over a 10 day forecast for 3 different experiments. The top panel is from a T106L19 experiment which corresponds to the operational forecast described above. The bottom panel is also from a T106L19 experiment but with modifications to the cloud scheme in the physics. The middle panel uses the same cloud scheme and physics as the bottom panel but has been run with 31 levels. This version is comparable with experiments run at T213 for which the diabatic increments are not available. Note that compared with the zonal mean temperature error plots, the North pole is now on the right. Also be wary of slightly different vertical scales on the axes in each of the panels.

The top panel in figure 17 reveals the marked cooling (over 1K per day) around 200hPa in the northern hemisphere thought to be responsible for the loss of PV. Interestingly, the change in the cloud scheme changes the cooling profile; the diabatic cooling in the bottom panel has its maximum at a slightly lower altitude and it is more spread out. The middle panel reveals a stronger cooling around the tropopause (e.g. around .2K per day in the southern hemisphere; the characteristic sloping of the tropopause upwards towards the equator looks realistic) showing that the cloud scheme and the rest of the physics are affected by the change in vertical resolution. The cooling regions just discussed are dominated by radiational cooling in the model.

At the end of this part of the trial of the T213L31 model, verification scores over the 18 cases run showed that the T213L31 model scored better than the T106L19 model during this (northern hemisphere) summer period.

Further scrutiny of PV maps form the operational T213L31 model during the southern hemisphere summer revealed a tendency for an increase in PV in the lower stratosphere. This was particularly noticeable at the

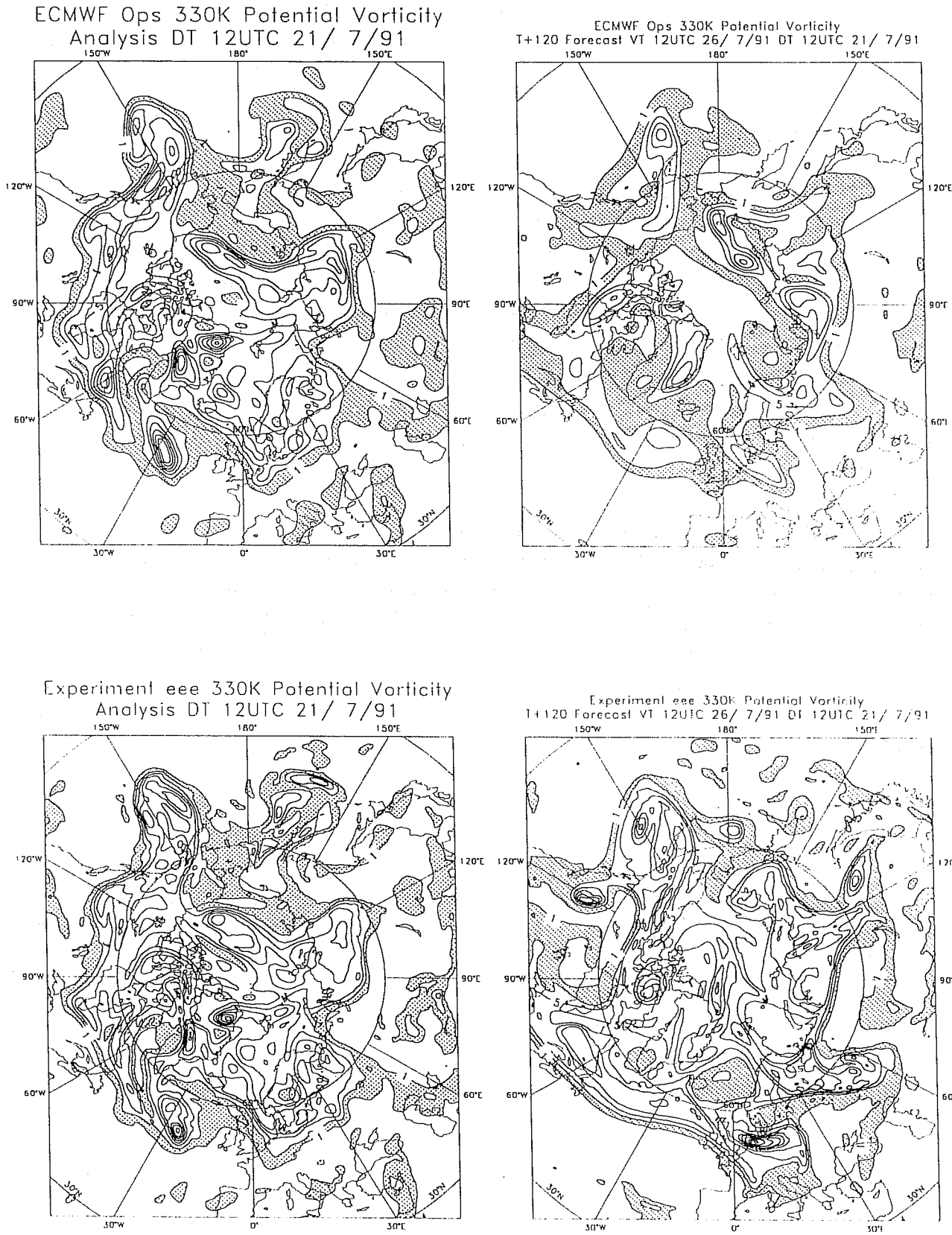

Fig.15. PV on the 330K surface, Northern hemisphere. Contours every 1 pvu, 1-2 units shaded.
Top panels: T106L19 cycle 36 analysis 12UTC 21/7/91 left; 5 day forecast right.
Bottom: T213L31 cycle 40 analysis 12UTC 21/7/91 left; 5 day forecast right.

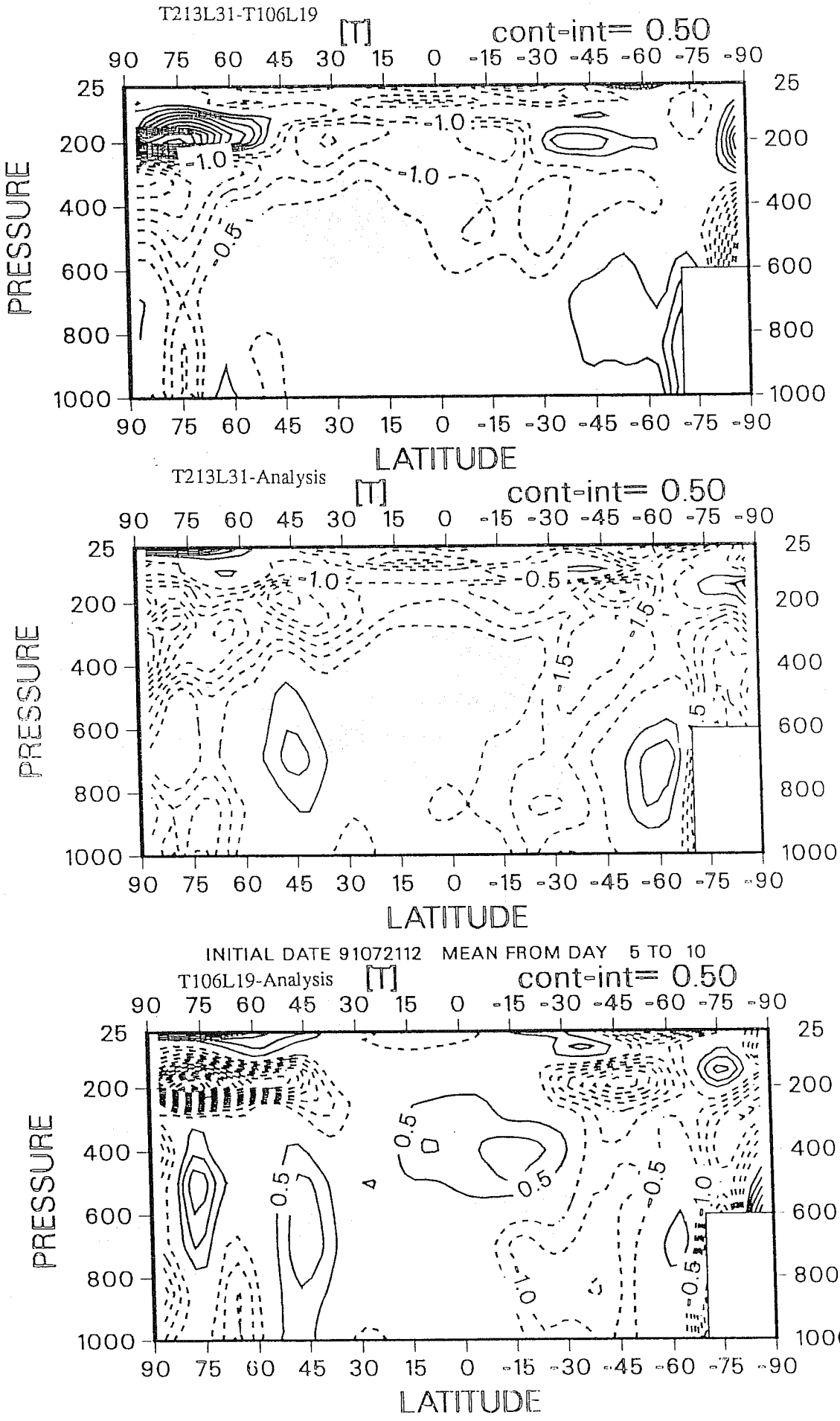

Fig.16. Zonal mean temperature. Mean 5-10 days. Forecasts from 12UTC 21/7/91.

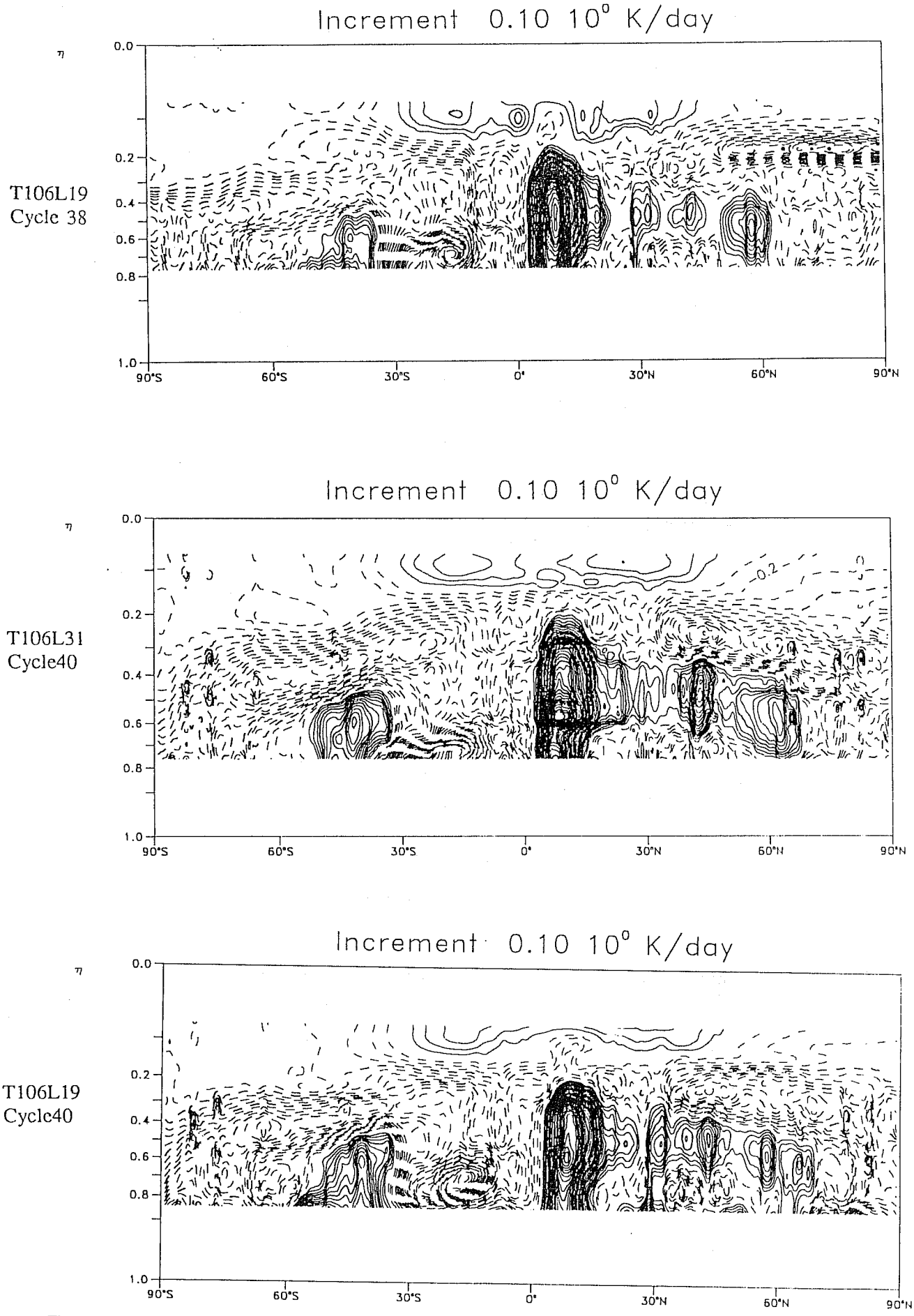

Fig.17. Total diabatic increments 0-10 days from 12UTC 21/7/91. Increments 0.1K per day, cooling dashed.

315K level. This behaviour was also detected in the northern hemisphere winter. The phenomena can be seen in figure 18 which shows a T106L19 analysis (top left) and 5 day forecast (top right) and the corresponding T213L31 operational plots on the bottom. The 5-6 pvu region has been shaded and it is apparent that the shaded area is greater in the 5 day forecast than in the analyses. Overall, the PV gradients also appear to be more intense in the forecasts. In this case there is no change in the vortex area at T213L31 but the region <-5pvu increases from 3% to 7% of the hemisphere. At T106L19 the vortex area reduces from 25% to 23% of the hemisphere and the region <-5pvu increases from 3% to 5% of the hemisphere.

Zonal mean temperature errors around the tropopause in figure 19 show a colder bias at T106L19 (bottom frame) than at T213L31 (middle frame); the difference in zonal mean temperature between T213L31 and T106L19 is shown in the top frame. However, diabatic increments in figure 20 show a greater diabatic cooling around the extra-tropical tropopause in the T106L31 level case (middle panel, about 1.3K maximum in the southern hemisphere) than in the T106L19 case (bottom panel, about 1K maximum in the southern hemisphere). This is believed to show a sensitivity of the physics parametrizations to vertical resolution; in particular to the cloud algorithm. The top panel shows the diabatic increments from the earlier version of the physics which was used operationally when the summer tests were carried out. The reason for the colder bias in the 19 level forecast is a reduction in the adiabatic poleward transport of heat. The stronger diabatic cooling in the 31 level forecast is more than compensated by a larger poleward transport of heat by the advection.

The increase in PV over the forecast may be responsible for the noticeable increase in the eddy kinetic energy in the model. Figure 21 shows a typical example in the southern hemisphere. The top panel shows the kinetic energy for wavenumbers 1 to 40 and the bottom panel shows the kinetic energy accounted for by wavenumbers 4-9, a typical range for synoptic waves. Typically KE levels at T106L19 are at or slightly lower than the analysis (full line) whereas those from 31 level forecasts are significantly higher. Similar, but less severe effects are detectable in the northern hemisphere forecasts and may account for the increased variability in the forecasts noticed last winter.

Cooling rates around the tropopause are largest in the vicinity of cloud tops. Figure 22 shows a plot of 24 hour temperatures changes due to the radiation processes from a T106L31 forecast from 12UTC 4/2/92 for model level 14 (around 350hPa). The contour interval is 2K and the dotted line represents cooling, the continuous line heating. The bottom panel shows the instantaneous cloud fraction at the same level for a time mid-way through the period at T+12. From inspection it can be seen that most of the regions of significant cooling correspond to the cloudy regions. The radiational changes at this level in the model dominate those from other processes in the extra-tropics.

9. CONCLUSIONS

PV maps can be used not only to interpret atmospheric and numerical model behaviour but also in investigations and validation of model behaviour. Routine display of PV maps on a suitable isentropic surface would appear to be useful in any forecasting environment. In the particular study described above, PV maps have been essential in unravelling the various, interacting processes influencing model behaviour.

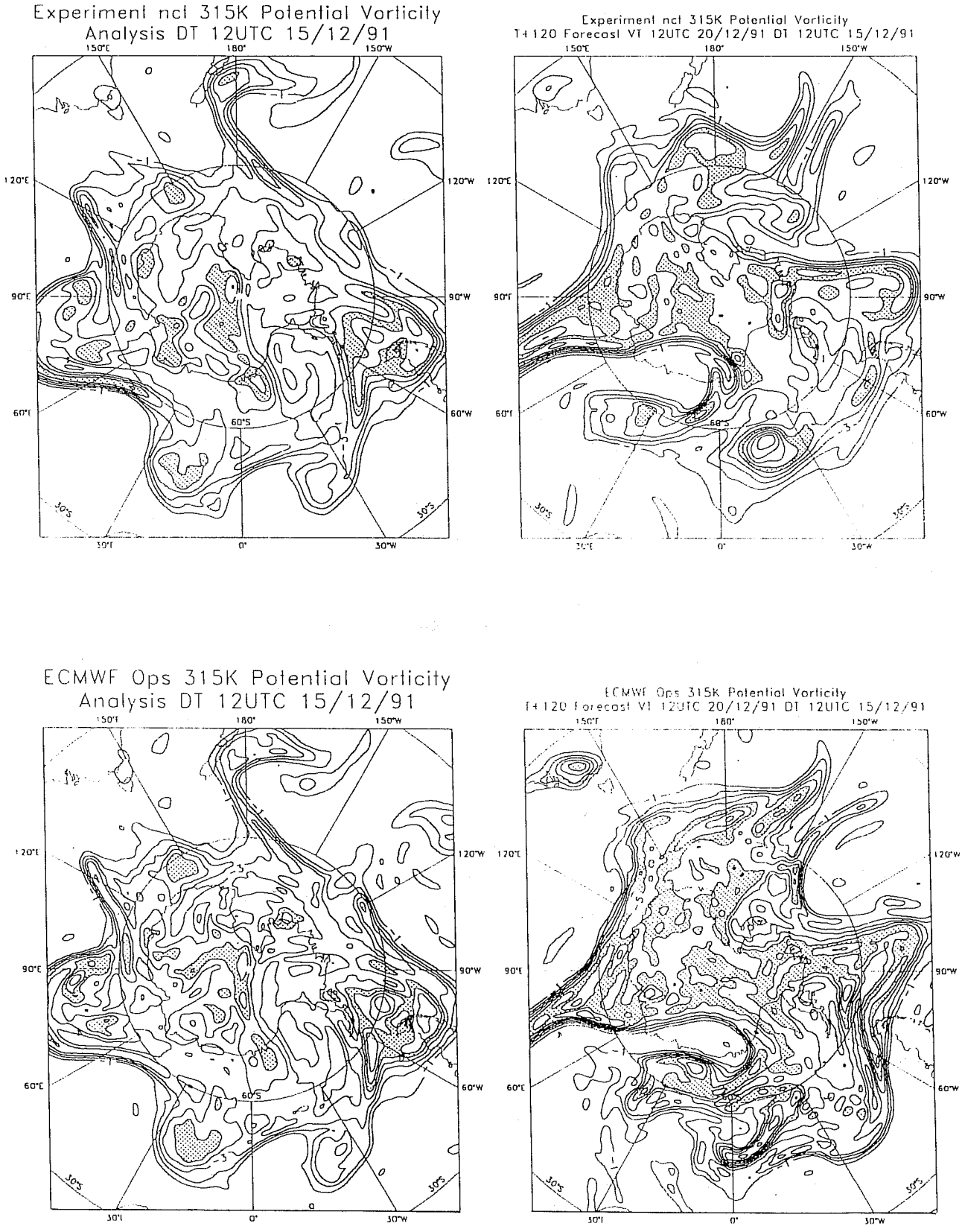

Fig.18. PV on the 315K surface, Southern hemisphere. Contours every 1pvu, -5 to -6 units shaded.
Top panels: T106L19 cycle 40 analysis 12UTC 15/12/91 left; 5 day forecast right.
Bottom: T213L31 cycle 40 analysis 12UTC 15/12/91 left; 5 day forecast right.

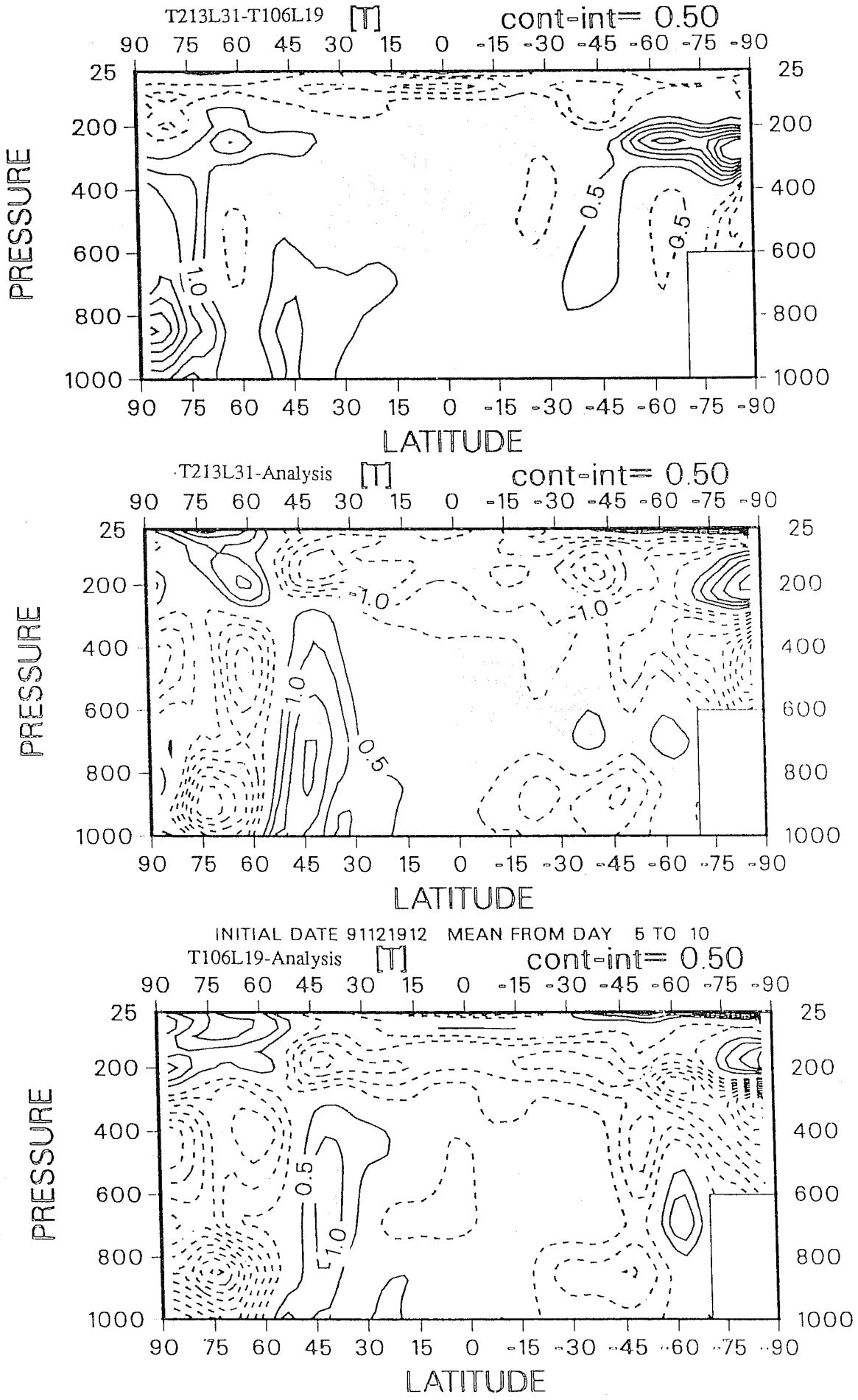

Fig.19. Zonal mean temperature. Mean 5-10 days. Forecasts from 12UTC 19/12/91.

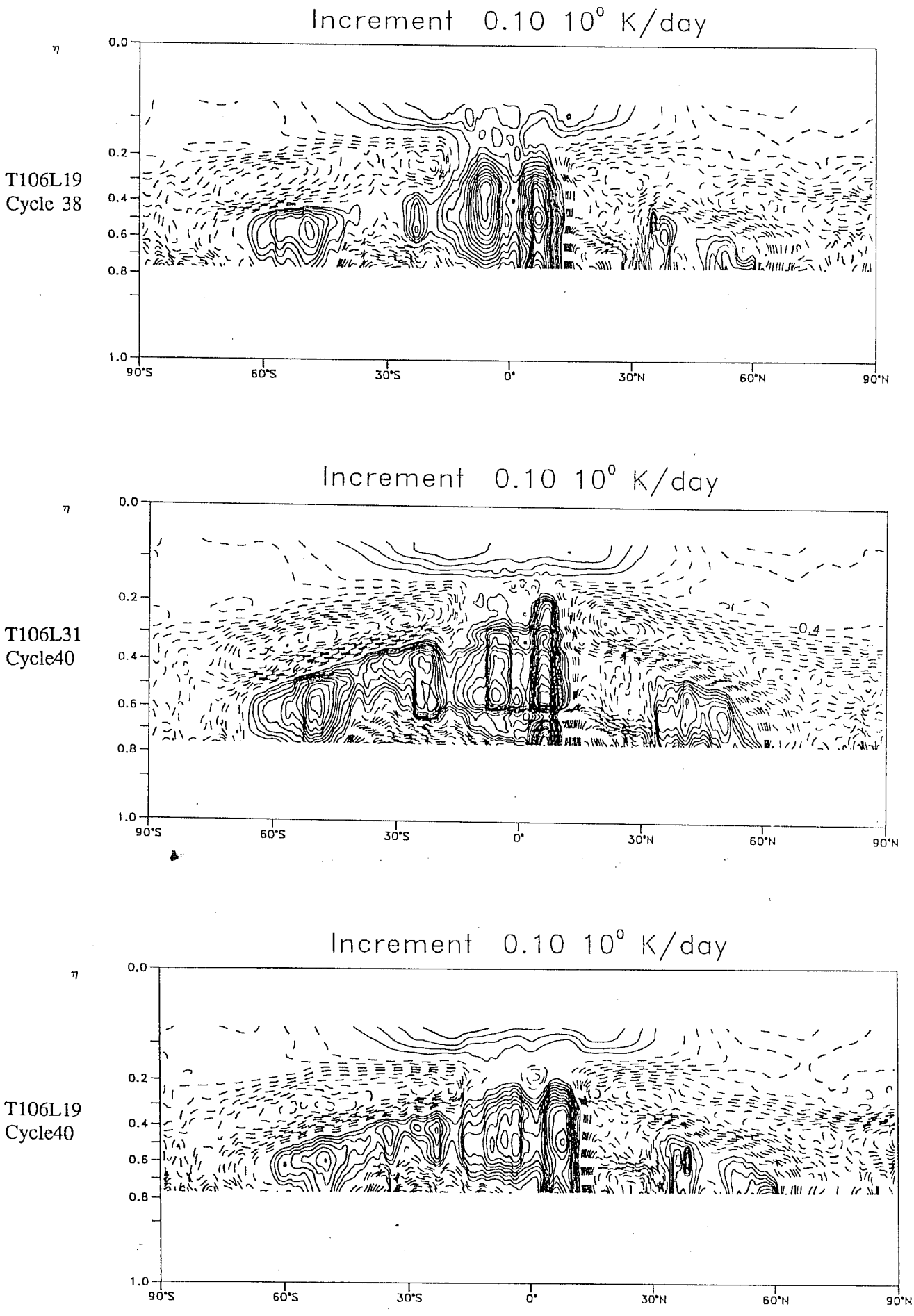

Fig.20. Total diabatic increments 0-10 days from 12UTC 15/12/91. Increments 0.1K per day, cooling dashed.

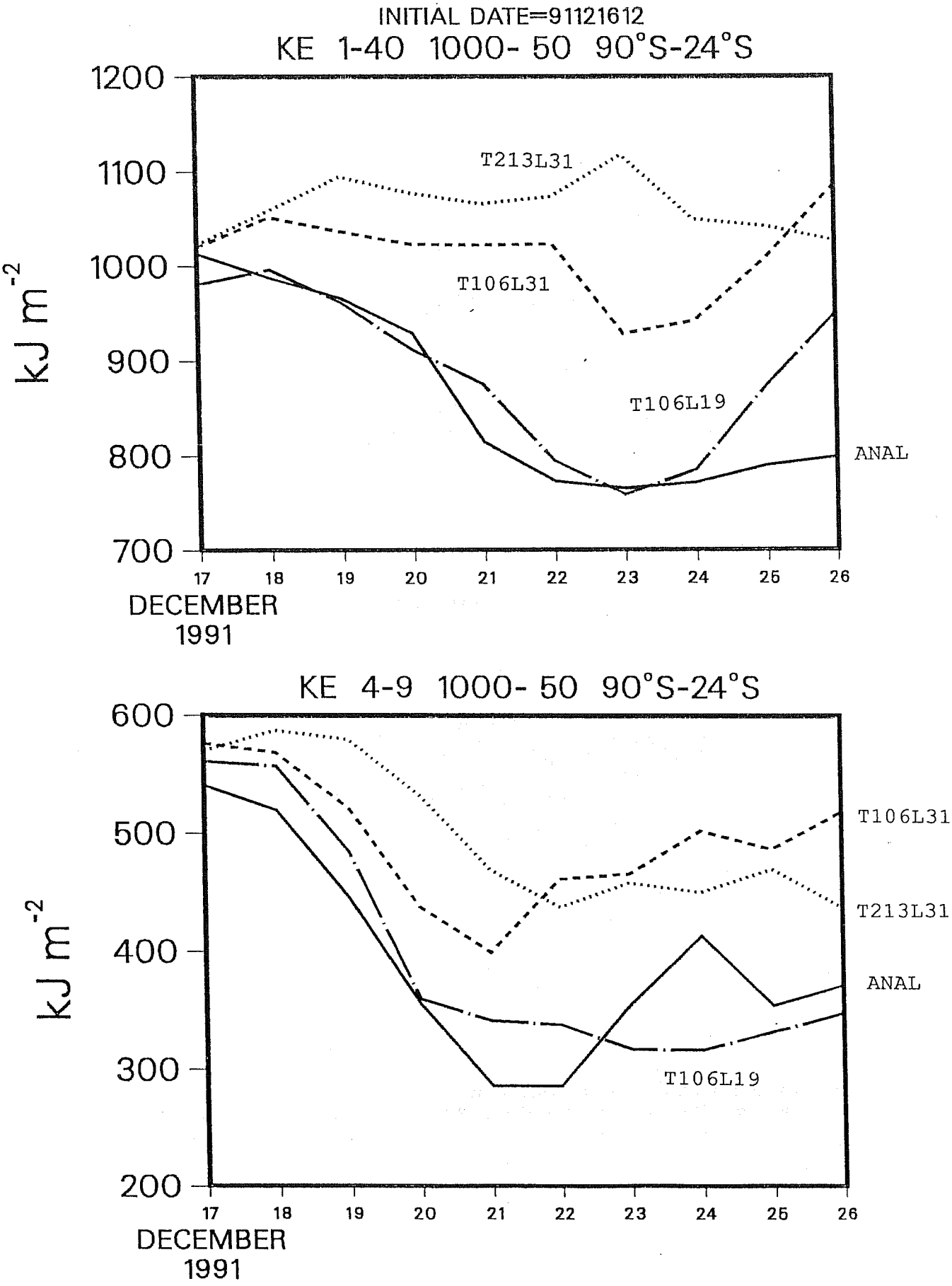

Fig.21. Eddy kinetic energy. Analyses between 12UTC 17/12/91 to 26/12/91 and forecasts from 16/12/91.

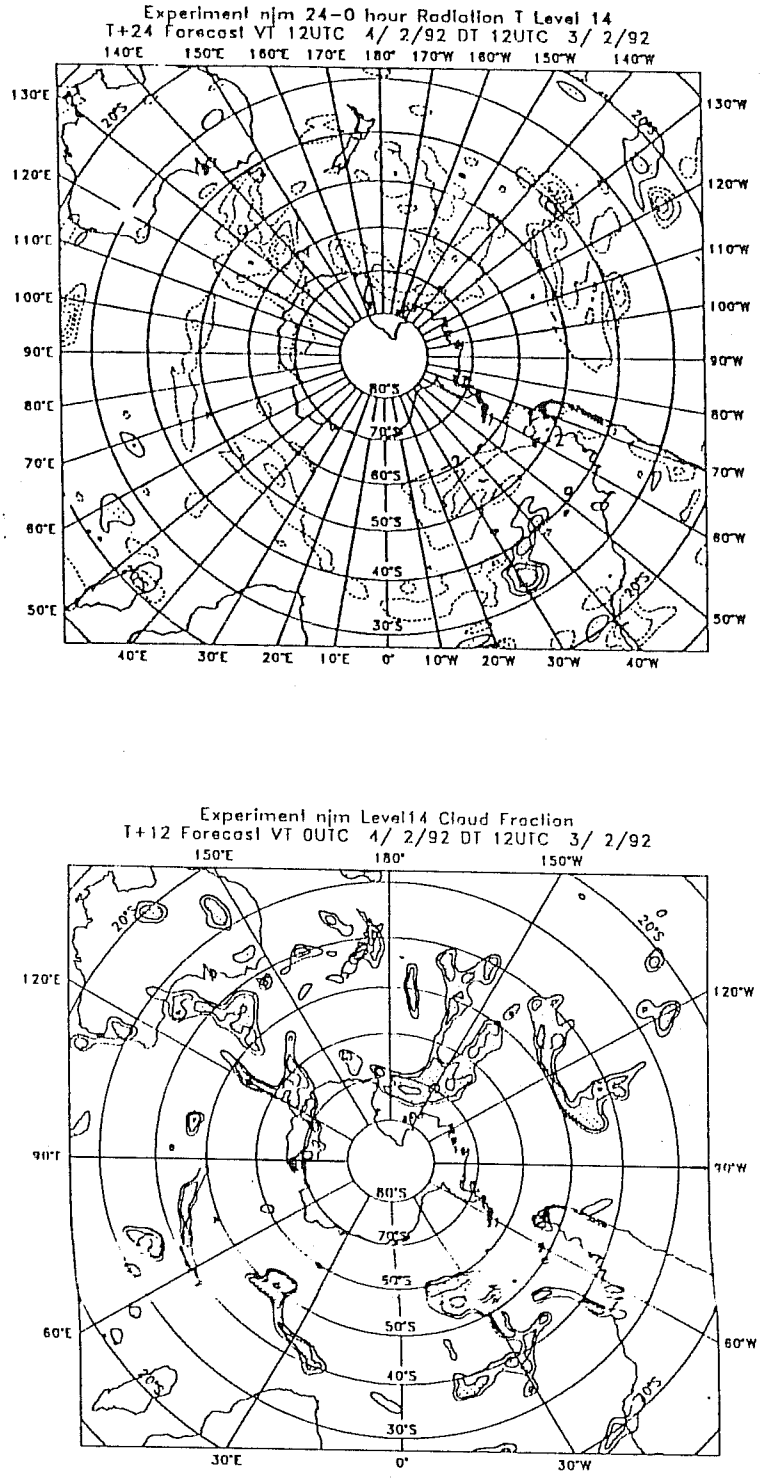

Fig.22. Top panel: Southern hemisphere temperature changes at level 14 (approximately 350hPa) due to radiation increments from a T106L31 24 hour forecast from 12UTC 3/2/92. Contours every 2K, cooling dashed. Bottom panel: Cloud fraction at T+12 of the above forecast (mid-time), 60% and 90% contoured. 1000hPa to 50hPa. 24°S-90°S. Wavenumbers 1-40 top panel. Wavenumbers 4-9 bottom panel.

REFERENCES

Crum, F.X. and D.E. Stevens, 1988: A case study of atmospheric blocking using isentropic analysis. Mon.Wea.Rev., 116, 223-241.

Dutton, J.A., 1986: The Ceaseless Wind. Dover Publications, 579pp.

Hoskins, B.J., M.E. McIntyre, and A.W. Robertson, 1985: On the use and significance of isentropic potential vorticity maps. Q.J.Roy.Meteor.Soc., 111, 877-946.

Hoskins, B.J., 1990: Theory of Extratropical Cyclones. Chapter 5. Extratropical Cyclones. The Erik Palmén Memorial Volume. Ed. by Newton, C.W. and E.O. Holopainen. American Meteorological Society, Boston, USA.

McIntyre, M.E., 1987: The dynamical significance of isentropic distributions of potential vorticity and low-level distributions of potential temperature. ECMWF Seminar on The Nature and Prediction of Extra Tropical Weather Forecasts, 7-11 September 1987, Vol 1, 237-259.

McIntyre, M.E., 1987: The use of potential vorticity and low-level temperature/moisture to understand extratropical cyclogenesis. ECMWF Seminar on The Nature and Prediction of Extra Tropical Weather Forecasts, 7-11 September 1987, Vol 1, 261-280.

Miles, M.K., 1959: Factors leading to the meridional extension of thermal troughs and some forecasting criteria derived from them. Met.Mag., 88, p193.

Thorpe, A.J., 1985: Diagnosis of balanced vortex structure using potential vorticity. J.Atmos.Sc, 42, p397-406.

Uccellini, L.W., 1990: Processes contributing to the rapid development of extratropical cyclones. Chapter 6. Extratropical Cyclones. The Erik Palmén Memorial Volume. Ed. by Newton, C.W. and E.O. Holopainen. American Meteorological Society, Boston.